63-3-2

ASD-TDR-62-492
Volume I

THEORETICAL INVESTIGATION OF A MAGNETO-OPTICAL GYROSCOPE

Faraday and Transit-time Effects

TECHNICAL DOCUMENTARY REPORT NO. ASD-TDR-62-492, Volume I

February 1963

Navigation and Guidance Laboratory
Aeronautical Systems Division
Air Force Systems Command
Wright-Patterson Air Force Base, Ohio

Project No. 4431, Task No. 443124

(Prepared under Contract No. AF33(616)-7668
by Electronic Systems Laboratory,
Department of Electrical Engineering,
Massachusetts Institute of Technology,
Cambridge 39, Massachusetts
Author: Richard B. Rothrock)

NOTICES

When Government drawings, specifications, or other data are used for any purpose other than in connection with a definitely related Government procurement operation, the United States Government thereby incurs no responsibility nor any obligation whatsoever; and the fact that the Government may have formulated, furnished, or in any way supplied the said drawings, specifications, or other data, is not to be regarded by implication or otherwise as in any manner licensing the holder or any other person or corporation, or conveying any rights or permission to manufacture, use, or sell any patented invention that may in any way be related thereto.

Qualified requesters may obtain copies of this report from the Armed Services Technical Information Agency, (ASTIA), Arlington Hall Station, Arlington 12, Virginia.

This report has been released to the Office of Technical Services, U.S. Department of Commerce, Washington 25, D.C., in stock quantities for sale to the general public.

Copies of this report should not be returned to the Aeronautical Systems Division unless return is required by security considerations, contractual obligations, or notice on a specific document.

74-563N, 300, 4-11-63

FOREWORD

This report was prepared by the Electronic Systems Laboratory, Massachusetts Institute of Technology, Cambridge 39, Massachusetts, on Air Force Contract AF-33(616)-7668 under Task No. 443124 of Project No. 4431 (formerly 50758 and 1 (620-4431), respectively.) The work was administered under the direction of the Navigation and Guidance Laboratory, Aeronautical Systems Division. Captain James E. Stevens (ASRNGC-2) was project engineer for the Navigation and Guidance Laboratory.

This report, in two volumes of which this is Volume I, is the Technical Documentary Report that constitutes Item II under Contract No. AF33 (616)-7668. The study covered by this report took place in the period November 1960 through October 1961. The contractor's report number is ESL-R-125(I).

The following professional staff members contributed to the research reported in this document:

R. Kramer	Project Engineer (to Feb. 1962)
G. C. Newton Jr.	Associate Professor of Electrical Engineering and Associate Director of the Electronic Systems Laboratory
P. S. Pershan	Consultant in Physics
R. B. Rothrock	Research Assistant

The principal author of this report is Richard B. Rothrock.

ABSTRACT

This report presents a study of magneto-optical and other closely related phenomena. The object of this study is to determine the sensitivity of these phenomena to angular motion in order to ascertain the feasibility of a "magneto-optical gyroscope."

The three phenomena studied are: (1) the optical Faraday effect, (2) the microwave Faraday effect, and (3) transit-time effects. Angular motion sensing instruments would utilize either of the first two effects in combination with the third. Throughout these studies it is assumed that the output signal is generated in response to the rotation of the plane of polarization of the detected radiation relative to that of the incident radiation.

It is found that the transit-time effects produce little rotation of the plane polarization, for a given angular rate, compared with that produced by the Faraday effect. Estimates for angular motion sensors that employ the optical and microwave Faraday effects show that the resolutions that could be expected, after considerable development, would be of the order of 0.1 radian per second. To get this resolution magnetic fields must be shielded from the device so that field fluctuations are kept down to the order of 10^{-9} gauss. In view of this low resolution and high sensitivity to stray magnetic fields, "magneto-optical gyroscopes" based on the Faraday effect do not seem to be a fruitful area for further research.

PUBLICATION REVIEW

This technical documentary report has been reviewed and is approved.

FOR THE COMMANDER:

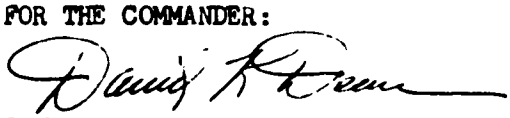

DAVID A. DEAN
Colonel, USAF
Chief, Navigation &
Guidance Laboratory

ASD-TDR-62-492, Vol. I

TABLE OF CONTENTS

CHAPTER I	INTRODUCTION AND SUMMARY	page	1
	A. Principles of Device		1
	B. Barnett Effect		2
	C. Angular Speed Threshold for Optical Faraday Gyro		3
	D. Angular Speed Threshold for Microwave Faraday Gyro		4
	E. Influence of Stray Magnetic Fields		4
	F. Transit-time Effects		4
	G. Conclusion		5
CHAPTER II	USE OF THE OPTICAL FARADAY EFFECT TO MEASURE MAGNETIC FIELDS		7
	A. Introduction		7
	B. Mechanical Vibration Model of Faraday-Effect Mechanism		7
	C. Signal-to-noise Ratio of Optical Faraday-Effect Magnetometer		12
	D. Estimate of Signal-to-noise Ratio Near Resonance		18
	E. Estimate of Signal-to-noise Ratio Off Resonance		21
CHAPTER III	USE OF THE MICROWAVE FARADAY EFFECT TO MEASURE MAGNETIC FIELDS		25
	A. Introduction		25
	B. Mechanism of Microwave Faraday Effect		25
	C. Resonance Effects		31
	D. Sensitivity of Microwave Magnetometer		32
CHAPTER IV	TRANSIT-TIME EFFECTS		37
	A. Transit-Time Effects in Isotropic Media		37
	B. Transit-Time Effects in Anisotropic Media		38

TABLE OF CONTENTS (continued)

APPENDIX A	MAGNITUDE OF FARADAY ROTATION IN DIFFERENT MATERIALS	page 43
	1. Gases	43
	2. Liquids	43
	3. Solids	44
APPENDIX B	ESTIMATE OF OPTICAL CONSTANTS FOR TYSONITE	48
APPENDIX C	PROPERTIES OF TYPICAL FERRITES	49
APPENDIX D	RELATION OF MINIMUM DETECTABLE FIELD TO MAGNETIC SENSITIVITY	50
APPENDIX E	INFLUENCE OF POLARIZER AND ANALYZER ON OPTICAL SENSITIVITY	51
APPENDIX F	USE OF MIRRORS TO INCREASE OPTICAL PATH	54
APPENDIX G	USE OF LASER AS LIGHT SOURCE	61
BIBLIOGRAPHY		64

CHAPTER I

INTRODUCTION AND SUMMARY

A. PRINCIPLES OF DEVICE

It is possible to detect mechanical rotation through its effect upon the transmission of electromagnetic waves through a material medium. It is the purpose of this memorandum to explore the effects of mechanical rotation upon the transmission characteristics of a material dielectric, and to estimate quantitatively the influence of mechanical rotation upon two specific phenomena: the optical Faraday effect and the microwave Faraday effect. An "optimistic" estimate will be made of the smallest angular rates that could be detected by devices based on the optical and microwave Faraday effects.

The Faraday effect concerns the rotation of the plane of polarization of linearly polarized electromagnetic waves upon transmission through a material dielectric in the presence of a magnetic bias field. The phenomenon can be detected by an apparatus consisting of a linearly polarized radiation source; the transmission medium with its associated magnetic field; a polarization analyzer at the output end of the transmission medium; and a detector to measure the strength of the radiation leaving the analyzer. If the Faraday effect is influenced by mechanical rotation, then the apparatus described above should indicate a change in the radiation intensity leaving the analyzer when the entire device is rotated.

The Faraday effect in a dielectric results from perturbations of the motions (or energy states) of atomic electrons within the dielectric, produced by the magnetic bias field. The result of mechanically rotating the transmission medium, in the form of additional perturbations of the electronic energy states, can most conveniently be estimated by representing the mechanical rotation by an equivalent magnetic field. This equivalence of mechanical rotation and magnetic field, in regard to their effects on the motions of atomic electrons within a dielectric, is discussed in the following section.

Manuscript released by the authors in October 1961 for publication as an ASD Technical Documentary Report.

B. BARNETT EFFECT

An atomic electron with angular momentum $\vec{J}$, attached to a rotating reference frame experiences a precession torque tending to force the electron angular momentum to precess about the angular velocity vector of the rotating reference frame. If $\vec{\Omega}$ is the angular velocity of the reference frame, then this precession torque is equal to $\vec{\Omega} \times \vec{J}$.

An electron circling around an atom in the presence of a magnetic field $\vec{H}$ also experiences a precession torque equal to $\vec{M} \times \vec{H}$, where $\vec{M}$ is the electron's magnetic moment. Since the electron's magnetic moment and angular momentum are colinear and are related by the gyromagnetic ratio, γ, as $\vec{M} = \gamma \vec{J}$, then the precession torque exerted on an electron by a magnetic field is equal to $\vec{M} \times \vec{H} = \gamma \vec{J} \times \vec{H} = -\gamma \vec{H} \times \vec{J}$. An equivalent result would be produced by mechanical rotation at an angular velocity $\vec{\Omega}$, provided that $\vec{\Omega}$ and $\vec{H}$ are related by

$$\vec{H} = -\frac{1}{\gamma}\vec{\Omega} \tag{1.1}$$

The gyromagnetic ratio, γ, would be equal to $\frac{e}{2m}$ for an electron whose angular momentum was due to orbital motion only, and would be $\frac{e}{m}$ if the angular momentum were due to spin alone. Generally an electron's total angular momentum results from a combination of orbital and spin momenta and its gyromagnetic ratio is $\frac{ge}{2m}$, where g is a dimensionless factor representing the way in which orbital and spin momenta are coupled. For Russell-Saunders coupling, the g-factor is:

$$g = \frac{3}{2} + \frac{S(S+1) - L(L+1)}{2J(J+1)} \tag{1.2}$$

where S, L and J are the electron's spin, orbit and total angular momentum quantum numbers, respectively. This type of coupling implies that the spin and orbital angular momenta are quantized separately and then added vectorially to produce the total angular momentum. The magnetic field equivalent to a rotational speed of $\vec{\Omega}$ radians per second is therefore

$$\vec{H}_{eq} = \frac{1.14}{g} \times 10^{-7} \vec{\Omega} \quad \text{oersteds} \qquad (1.3)$$

This equivalence between mechanical rotation and magnetic field strength was first demonstrated experimentally by S. J. Barnett.[14, 15, 16]*

Because of the relationship 1.3 between mechanical rotation and magnetic field strength in regard to their effects on electronic energy levels, it is possible to consider a "Faraday effect gyroscope" as basically a magnetometer. Using the relatively large amount of published data relating Faraday rotation to magnetic field intensity, the smallest magnetic field increments that might be detected by magnetometers based on the optical and microwave Faraday effects are estimated in Chapters II and III. In the following two sections these estimates of magnetic field thresholds are translated directly into equivalent angular rate thresholds for gyroscopic instruments by means of Eq. 1.3.

C. ANGULAR SPEED THRESHOLD FOR OPTICAL FARADAY GYRO

In Chapter II it is estimated that the best material to use as a transmission medium in constructing an optical Faraday-effect gyroscope is tysonite. In this mineral the large Faraday rotation is produced principally by the Ce^{3+} ions. Assuming then that the equivalent Barnett-effect field which would represent the response of the Faraday rotation in a tysonite crystal to mechanical rotation is that field which would be produced by rotating the Ce^{3+} ions alone, the "g" factor to be used in Eq. 1.3 above is $g \approx 1$. The magnetic field threshold for an optical Faraday effect magnetometer using a tysonite crystal at $4^{\circ}K$ is estimated in Chapter II as 6×10^{-9} oersteds. Using this magnetic field in Eq. 1.3 gives a corresponding minimum detectable angular rate of

$$\vec{\Omega}(0 \text{ db}) = 5 \times 10^{-2} \text{ radians/second} \qquad (1.4)$$

---

* Superscripts refer to numbered items in the Bibliography.

D. ANGULAR SPEED THRESHOLD FOR MICROWAVE FARADAY GYRO

In Chapter III it is estimated that the smallest detectable magnetic field increment for a microwave Faraday effect magnetometer operating at room temperature is 4×10^{-8} oersteds. Using this magnetic sensitivity threshold, with a "g" factor of 2 for ferrimagnets, gives a minimum detectable angular rate of

$$\vec{\Omega} = 0.35 \quad \text{radians/second}$$

E. INFLUENCE OF STRAY MAGNETIC FIELDS

The magnetic field thresholds for the optical and microwave Faraday-effect instruments discussed in Chapters II and III arise from limitations imposed by noise sources in them. These threshold estimates do not include allowances for the effects of stray magnetic fields. The equivalence of mechanical rotation and magnetic field is meaningless unless the instrument can be shielded from external magnetic interference to at least the same order of magnitude as those fields corresponding to the smallest angular rates that it is desired to detect. The magnetic field equivalent to the angular rate threshold of 5×10^{-2} radians/second estimated for the optical Faraday effect device was 6×10^{-9} oersteds. For the microwave Faraday effect device, with an estimated angular rate threshold of 0.35 radian/second at room temperature, the equivalent magnetic field is about 10^{-8} oersted. It is quite obvious that providing magnetic shielding to this degree is a major problem in such a device.

F. TRANSIT-TIME EFFECTS

Chapter IV discusses transit time effects on the plane of polarization of light transmitted through a rotating medium. Even in the absence of the Faraday effect some rotation will occur because of the finite time required for radiation to pass through the medium. However, it is shown that the resolution of a device that depends solely on transit time is of the order of one ten thousandth of that estimated for devices that employ the Faraday effect.

G. CONCLUSION

The resolution estimates given in Sections C and D above, for angular motion sensors based upon the Faraday effect are in the vicinity of 0.1 radian per second for the minimum detectable angular rate. This figure applies to both optical and microwave devices. It is an optimistic figure in the sense that considerable research and development would be necessary to realize it. Mechanical gyroscopes are able to achieve resolutions orders of magnitude better than 0.1 radian per second. Therefore it is concluded that further exploration of the magneto-optical gyro based on the Faraday effect is not warranted at this time.

CHAPTER II

USE OF THE OPTICAL FARADAY EFFECT TO MEASURE MAGNETIC FIELDS

A. INTRODUCTION

Michael Faraday, in 1845, discovered that pieces of heavy glass placed in a strong magnetic field would rotate the plane of polarization of linearly polarized light transmitted through the glass in the direction of the magnetic field.[19] He regarded this as firm experimental evidence of a connection between magnetism and light, and subsequently detected the same effect in several other transparent solids and liquids. The Faraday effect has since been observed in nearly all types of materials. Verdet concluded from experimental measurements that the Faraday rotation of the plane of polarization is proportional to the path length of light through the material and to the magnetic field strength (if the material is not near magnetic saturation):

$$\phi = VLH$$

where ϕ is the total Faraday rotation through the material, L is the length of material and H is the magnetic field strength. The proportionality factor V is called Verdet's constant, and is a function of the frequency of light used and the temperature (i.e., magnetic susceptibility) of the material as well as the type of material. Typical values of Verdet's constant for different types of materials are listed in Appendix A.

B. MECHANICAL VIBRATION MODEL OF FARADAY-EFFECT MECHANISM

An exact analysis of the Faraday effect and accurate calculation of the Verdet constant for different materials requires a quantum mechanical treatment. However, the phenomenon can be interpreted roughly in terms of a classical mechanical vibration analog which helps in visualizing the operation of the effect and gives, within an order of magnitude, the size of the Verdet constant in some simple cases. The mechanical vibration model, described below, is discussed in many texts on classical optics.[20, 21]

Imagine a particle of charge q and mass m attached to its rest position by a spring, of spring rate K. If there is also a large constant magnetic field $\vec{B}$ in the region, directed along the +z axis, and alternating electric field components E_x and E_y, then the differential equations of motion of the particle are:

$$\begin{aligned} m\ddot{x} + Kx &= q E_x + q B\dot{y} \\ m\ddot{y} + Ky &= q E_y - q B\dot{x} \end{aligned} \tag{2.1}$$

Forces on the particle due to its motion within the magnetic field associated with the time-varying E-field have been assumed to be negligible compared to those caused by the large constant field $\vec{B}$, and all forms of energy dissipation have been neglected. If x(t), y(t), $E_x(t)$ and $E_y(t)$ are assumed to be sinusoidal time functions with complex amplitudes given by:

$$\begin{aligned} x(t) &= \mathrm{Re}\left[\hat{x}\, e^{j\omega t}\right] \\ y(t) &= \mathrm{Re}\left[\hat{y}\, e^{j\omega t}\right] \\ E_x(t) &= \mathrm{Re}\left[\hat{E}_x\, e^{j\omega t}\right] \\ E_y(t) &= \mathrm{Re}\left[\hat{E}_y\, e^{j\omega t}\right] \end{aligned} \tag{2.2}$$

then substituting these expressions into Eq. 2.1 gives the complex amplitudes $\hat{x}$ and $\hat{y}$ as

$$\begin{aligned} \hat{x} &= C\hat{E}_x + j D\hat{E}_y \\ \hat{y} &= -j D\hat{E}_x + C\hat{E}_y \end{aligned}$$

where

$$C = \frac{\frac{q}{m}(\omega_o^2-\omega^2)}{(\omega_o^2-\omega^2)^2 - \frac{\omega^2 q^2 B^2}{m^2}} \quad \text{and} \quad \omega_o^2 = \frac{k}{m}$$

$$D = \frac{(\frac{\omega q^2 B}{m^2})}{(\omega_o^2-\omega^2)^2 - \frac{\omega^2 q^2 B^2}{m^2}} \tag{2.3}$$

The electric field must satisfy Maxwell's equations:

$$\nabla^2 \vec{E} = \mu \frac{\partial \vec{J}}{\partial t} \tag{2.4}$$

where $\vec{J}$ is the total current density. If there are N vibrating particles per unit volume,

$$\vec{J} = \epsilon \frac{\partial \vec{E}}{\partial t} + (Nq)\ (\text{Velocity of vibrating particle}),\ \text{or}$$

$$J_x = \epsilon \frac{\partial E_x}{\partial t} + Nq\dot{x}$$

$$J_y = \epsilon \frac{\partial E_y}{\partial t} + Nq\dot{y} \tag{2.5}$$

Substituting expressions 2.2 and 2.3 for x and y:

$$\nabla^2(\hat{E}_x e^{j\omega t}) = \mu(\epsilon + NqC)\frac{\partial^2}{\partial t^2}(\hat{E}_x e^{j\omega t}) + j\mu NqD\frac{\partial^2}{\partial t^2}(\hat{E}_y e^{j\omega t})$$

$$\nabla^2(\hat{E}_y e^{j\omega t}) = \mu(\epsilon + NqC)\frac{\partial^2}{\partial t^2}(\hat{E}_y e^{j\omega t}) - j\mu NqD\frac{\partial^2}{\partial t^2}(\hat{E}_x e^{j\omega t}) \tag{2.6}$$

For an electromagnetic wave circularly polarized in the (+z) sense, the electric field components are related by:

$$\hat{E}_x = + j \hat{E}_y$$

$$\hat{E}_y = - j \hat{E}_x \tag{2.7}$$

and substituting these relations into Eq. 2.6:

$$\nabla^2 (\hat{E}_x e^{j\omega t}) = \mu(\epsilon + NqC + NqD) \frac{\partial^2}{\partial t^2} (\hat{E}_x e^{j\omega t})$$

$$\nabla^2 (\hat{E}_y e^{j\omega t}) = \mu(\epsilon + NqC + NqD) \frac{\partial^2}{\partial t^2} (\hat{E}_y e^{j\omega t}) \tag{2.8}$$

So the propagation velocity for a (+z) circularly polarized wave is:

$$\left(\frac{1}{V^+}\right)^2 = \mu(\epsilon + NqC + NqD) \tag{2.9}$$

For a circularly polarized wave rotating in the (-z) sense, the electric field components are related by

$$\hat{E}_x = - j \hat{E}_y$$

$$\hat{E}_y = + j \hat{E}_x \tag{2.10}$$

and the propagation velocity, found by substituting Eq. 2.10 into Eq. 2.6 is:

$$\left(\frac{1}{V^-}\right)^2 = \mu(\epsilon + NqC - NqD) \tag{2.11}$$

If a linearly polarized wave incident upon this dielectric is regarded as being split into positive and negative circularly polarized components of equal amplitude, these circularly polarized components will then travel at

the velocities given by Eqs.2.9 and 2.11. After traveling a distance L through the dielectric, the linearly polarized wave resulting from the superposition of the oppositely rotating circularly polarized components will have its polarization direction shifted from its initial polarization by an angle ϕ, given by:

$$\phi = \frac{1}{2} L\omega \left(\frac{1}{V^+} - \frac{1}{V^-}\right) \tag{2.12}$$

From Eqs.2.10 and 2.12,

$$\left(\frac{1}{V^+}\right)^2 - \left(\frac{1}{V^-}\right)^2 = \left(\frac{1}{V^+} + \frac{1}{V^-}\right)\left(\frac{1}{V^+} - \frac{1}{V^-}\right) = 2\mu NqD \tag{2.13}$$

Assuming that $\left(\frac{1}{V^+}\right)$ and $\left(\frac{1}{V^-}\right)$ are nearly equal so that

$$\left(\frac{1}{V^+} + \frac{1}{V^-}\right) \approx \frac{2n}{c}$$

where n = index of refraction

c = 3×10^8 meters per second

Then Eq. 2.13 gives $$\frac{2n}{c}\left(\frac{1}{V^+} - \frac{1}{V^-}\right) = 2\mu NqD$$

or $$\left(\frac{1}{V^+} - \frac{1}{V^-}\right) = \frac{\mu NqDc}{n}$$

and substituting into Eq. 2.12:

$$\phi = \frac{L\omega\mu Nq\,c\,D}{2n}$$

with D given in Eq. 2.3, so

$$\phi = \frac{L\omega^2 q^3 \mu N B c}{2n\left[(\omega_o^2-\omega^2)^2 - \frac{\omega^2 q^2 B^2}{m^2}\right] m^2} \qquad (2.14)$$

Neglecting $\frac{\omega^2 q^2 B^2}{m^2}$ for small fields and for $\omega \neq \omega_o$, and writing $B = \mu H$, Verdet's constant is:

$$V = \frac{\phi}{LH} = \frac{\omega^2 q^3 \mu^2 N c}{2m^2 n (\omega_o^2-\omega^2)^2} \qquad (2.15)$$

The preceding discussion suggests qualitatively why the Faraday effect should be expected to occur, if the vibrating charged particles are considered to be electrons. Formula 2.15 gives the right order of magnitude for Verdet's constant in cases where the interactions between adjacent electrons are small and where energy dissipation mechanisms are negligible, i.e., for gases at low pressure and away from resonance frequencies, provided the Faraday rotation is produced by one prominent resonance (ω_o). The same treatment may be modified, by the inclusion of empirical damping terms and the consideration of several resonance frequencies, to apply to more general cases.

C. SIGNAL-TO-NOISE RATIO OF OPTICAL FARADAY-EFFECT MAGNETOMETER

An estimate of the minimum magnetic field strength detectable with a Faraday effect magnetometer requires first the calculation of its signal-to-noise ratio. The type of device that will be assumed for this calculation is shown in Fig. 1.

A well-regulated light source supplies light of intensity I_1 to each of two identical crystal sections, which are placed in the magnetic field H that is to be measured. The incident light is polarized before entering the crystals, within which Faraday rotation of the direction of polarization takes

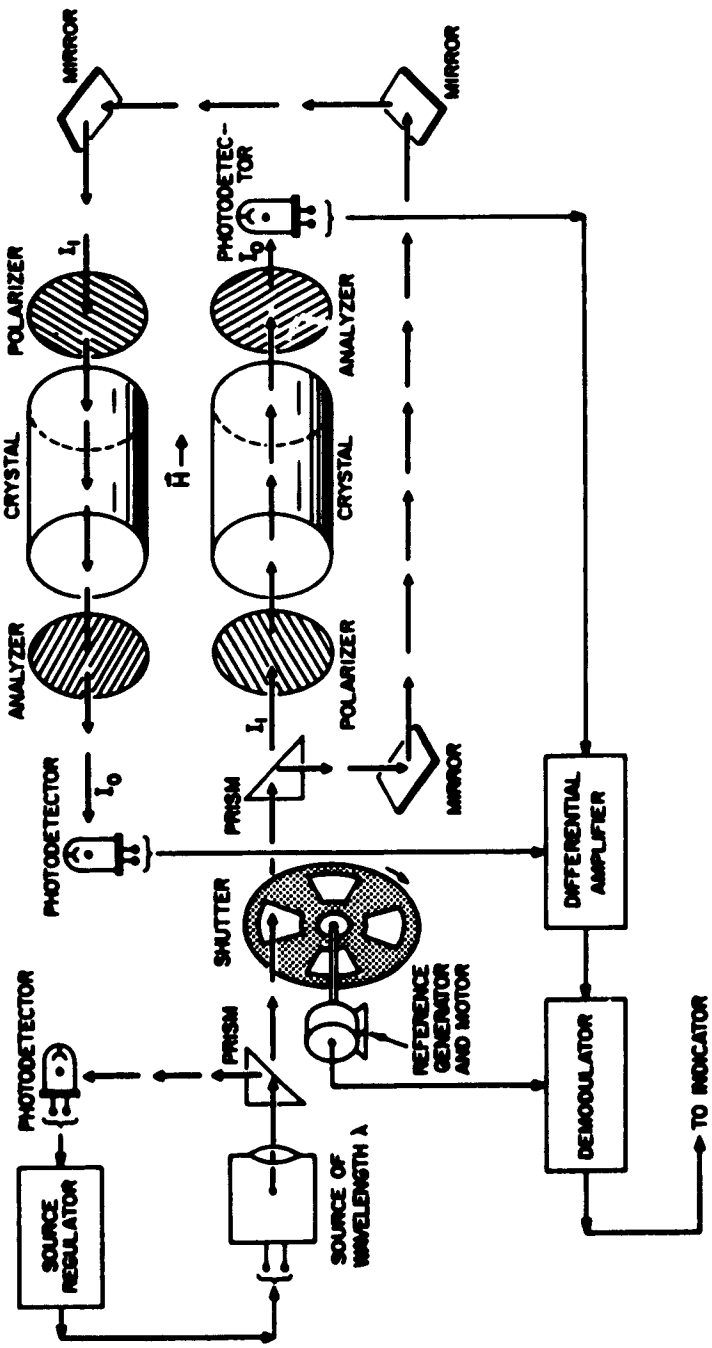

Fig. 1 Faraday-Effect Magnetometer

place, depending on the component of magnetic field along the crystal axes. After leaving the crystals the light beams pass through additional polarizing filters serving as analyzers which transmit a component, I_o, of the light beam to the photodetectors. The angular displacement of the polarizers and analyzers away from the setting for minimum transmission is ϕ_o, and the residual transmission through one polarizer and analyzer when adjusted for minimum transmission is τ_o. Since the light beams traverse the two crystal sections in opposite directions, a small component of H along the crystal axes will cause an increase in the transmission through one analyzer and a decrease in the other. This differential signal is sensed by the photodetectors and amplified to indicate the strength of the magnetic field. An AC coupled amplifier is desirable to avoid zero-drift problems, and consequently a shutter is included to modulate the light beam.

The remainder of this section is concerned with computing the output signal from the photodetectors as a function of magnetic field intensity along the crystal axes, evaluating noise sources within the system, and estimating the smallest magnetic field that could be detected based on the best choice of the free parameters of the device. The signal-to-noise ratio that is calculated is that at the photodetector outputs. Any electronics that might be connected to the detector outputs (an amplifier and demodulator are indicated in Fig. 1) can only degrade the signal-to-noise ratio further, and these possible effects will not be considered except to assume an overall bandwidth of ten cycles. Assuming the polarizers reduce the incident randomly-polarized light intensity by $(\frac{1}{2})$, then

$$\frac{I_o}{I_1} = \frac{1}{2} e^{-\alpha L} \left[\tau_o + \sin^2 (V L H + \phi_o)\right] \qquad (2.16)$$

where α is the attenuation per unit length through the crystal and V is the Verdet constant for the crystal (both α and V are functions of λ). A desirable material for use as the transmission medium should have a large Verdet constant and small attenuation. Consideration of the Verdet constants

for different materials given in Appendix A indicates that tysonite is a good choice. It is a mineral containing cerium and lanthanum, with small amounts of other rare earths, and flourine.[25] It has a large Verdet constant at low temperatures, and is transparent in the visible light range. From Eq. 2.16, the sensitivity of output light intensity to a change in magnetic field strength is

$$\left(\frac{1}{I_1}\right) \frac{dI_o}{dH} = \frac{1}{2} (V L e^{-aL}) (\cos 2\phi_o \sin 2VLH + \sin 2\phi_o \cos 2VLH) \tag{2.17}$$

At frequencies for which the Verdet constant, V, is high the absorption per unit length of crystal is also very high so that the useful length of crystal, L, is small. Consequently, if the magnetic field increments to be measured are small, then the total Faraday rotation through the crystals, VLH, is small even though the device may operate at frequencies where V is large (i.e., at resonance). If also $VLH \ll \phi_o$, then in Eq. 2.17, $\cos 2\phi_o \sin 2VLH \ll \sin 2\phi_o \cos 2VLH$, and $\cos 2VLH \approx 1$, so Eq. 2.17 simplifies to

$$\frac{dI_o}{dH} = \frac{1}{2} I_1 e^{-aL} VL \sin 2\phi_o \tag{2.18}$$

The noise at the output of the photodetector will next be estimated as a means for calculating the smallest increment of magnetic field strength that could be reliably detected. For this purpose the detector itself will be considered to be a photoemissive device only. Any current gain and additional noise that may be present in an actual detector (e.g., a photomultiplier) will be considered as part of the amplifier characteristics, and can only degrade the signal-to-noise ratio predicted for the output of the photoemissive device. The noise sources important in determining this signal-to-noise ratio are:

1. Detector noise
2. Fluctuations in light source intensity

In addition to these, thermal effects within the crystal may produce a random fluctuation of the Faraday rotation about its mean value. Information about the magnitude of such fluctuations has not been found; because of the low temperature at which the device would be operated ($\sim 10^{o}K$) this effect will be assumed to be negligibly small compared to the other noise sources.

At low temperatures the thermal emission from a photocathode will be much smaller than the shot noise; therefore the noise current generated in the detector is

$$i_{ND} = \text{RMS shot noise current} = (2\, e\, i_o\, \Delta F)^{1/2}$$

where e = electronic charge

i_o = zero-signal detector current

ΔF = frequency band within which the noise current is measured

Assuming that the detector has no dark current, the zero-signal detector current is $i_o = R I_b$, where R is the radiant sensitivity of the photocathode and I_b is the background intensity transmitted through the optical system in the absence of a magnetic field. Making this substitution:

$$i_{ND} = (2\, e\, R\, I_b\, \Delta F)^{1/2} \text{ amperes RMS} \qquad (2.19)$$

Another source of noise arises from fluctuations in the intensity of the light source. It is estimated that a well regulated light source would produce an RMS fluctuation in light intensity equal to about 10^{-8} times its mean intensity per cps of bandwidth, with a flat power spectrum out to a limiting frequency determined by the bandwidth of the regulator, which will be assumed to be greater than the bandwidth ΔF of the photodetector-amplifier-servo combination connected to the magnetometer. If a balanced detector and differential amplifier system is used (as indicated in Fig. 1) with 40 db rejection of common-mode signals, then the effective detector noise current produced by fluctuations of the light source is

$$i_{NS} = 10^{-12} R I_b \Delta F \text{ amperes RMS} \tag{2.20}$$

The background intensity striking the detector, I_b, which appears in Eqs. 2.19 and 2.20, is computed from Eq. 2.16 as

$$I_b = I_1 \left(\frac{1}{2} e^{-\alpha L}\right) (\tau_o + \sin^2 \phi_o) \tag{2.21}$$

The total noise current at the detector output can be obtained from Eqs. 2.19 and 2.20, assuming the two component noise currents to have independent Gaussian amplitude-probability distributions:

$$i_N = \left[R I_b \Delta F (2e + 10^{-24} R I_b \Delta F)\right]^{1/2}$$

The term $(R I_b)$ represents the zero-signal current output of the photodetector, and for linear operation of the device the free parameters should be chosen so that $R I_b$ does not exceed the linear range of the photocathode. The output current of a photocathode of one inch diameter becomes a noticeably less-than-linear function of incident light intensity at an output current of about 20 microamperes.[26] Assuming a bandwidth ΔF of ten cycles, then $10^{-24} R I_b \Delta F \ll 2e$, so the detector noise current is essentially equal to the shot noise component:

$$i_N = (2 e R I_b \Delta F)^{1/2} \tag{2.22}$$

The signal current leaving the photodetector (i_s) is obtained from Eq. 2.18, for small values of H:

$$\frac{1}{H} i_s = \frac{1}{2} I_1 RVL e^{-\alpha L} \sin 2\phi_o \tag{2.23}$$

The (current) signal-to-noise ratio, from Eqs. 2.22 and 2.23, is

$$\frac{1}{H} \frac{i_s}{i_N} = \frac{I_1 RVL e^{-\alpha L} \sin 2\phi_o}{2(2e R I_b \Delta F)^{1/2}} \tag{2.24}$$

Substituting Eq. 2.21 for I_b and assuming a bandwidth of ten cycles:

$$\frac{1}{H}\,\frac{i_s}{i_N} = 5.6\times10^{8}\, VL(R\,I_b)^{1/2}\,\frac{\sin 2\,\phi_o}{\tau_o + \sin^2\phi_o} \qquad (2.25)$$

Practical considerations governing the choice of parameters in Eq. 2.25 are different for wavelengths near an optical resonance than for wavelengths removed from any resonances. The following paragraphs estimate the greatest signal-to-noise ratio that could be achieved under each of these two conditions.

D. ESTIMATE OF SIGNAL-TO-NOISE RATIO NEAR RESONANCE

At wavelengths near an optical absorption line of the crystal, the attenuation is quite high. Therefore the photodetector zero-signal current ($R\,I_b$) would probably be below the saturation level, and Eq. 2.21 may be used to express I_b in terms of the other system parameters. Making this substitution in Eq. 2.25 gives:

$$\frac{1}{H}\,\frac{i_s}{i_N} = 7.8\times10^{8}\,(I_1 R)^{1/2}\left(\frac{V}{a}\right)\left(\frac{a\,L}{2}\,e^{-\frac{aL}{2}}\right)\frac{\sin 2\phi_o}{(\tau_o + \sin^2\phi_o)^{1/2}} \qquad (2.26)$$

The signal-to-noise ratio is apparently the largest, as a function of crystal length L, when L is chosen such that

$$\frac{a\,L}{2} = 1 \qquad (2.27)$$

Making this choice for crystal length, the signal-to-noise ratio is:

$$\frac{1}{H}\,\frac{i_s}{i_N} = 7.8\times10^{8}\left(\frac{1}{e}\right)(I_1 R)^{1/2}\left(\frac{V}{a}\right)\frac{\sin 2\phi_o}{(\tau_o + \sin^2\phi_o)^{1/2}} \qquad (2.28)$$

Assuming that $\tau_o << 1$, the factor in Eq. 2.28 involving ϕ_o has a maximum value of about 2 over the range of ϕ_o for which $\tau_o << \sin^2\phi_o << 1$. Using $\tau_o = 4x10^{-6}$ and $\phi_o = 10^{-2}$ radians, Eq. 2.28 becomes

$$\frac{1}{H}\frac{i_s}{i_N} = 5.7x10^8 (I_1 R)^{1/2} \left(\frac{V}{a}\right) \qquad (2.29)$$

In the vicinity of an active resonance line, the factor $\left(\frac{V}{a}\right)$ in Eq. 2.29 is a sensitive function of wavelength, and the operating frequency should be chosen to maximize this ratio. The following expressions for $a(\lambda)$ and $V(\lambda)$ can be obtained from an analysis similar to that of Section B, except that damping is considered.[20]

$$a(\lambda) = \frac{4\pi M G \lambda^2}{2n\left[(\lambda^2-\lambda_o^2)^2 + G^2\lambda^2\right]}$$

$$V(\lambda) = B\lambda \frac{dn}{d\lambda} \qquad (2.30)$$

where $n(\lambda)$ is the real part of the index of refraction, and is given by

$$n^2(\lambda) = 1 + \frac{M\lambda^2(\lambda^2-\lambda_o^2)^2}{(\lambda^2-\lambda_o^2)^2 + G^2\lambda^2} \qquad (2.31)$$

The constants are:

$B = 3x10^{-4}$ radians/cm-oersted

G = line width between half-power points of absorption line

M = material constant

λ_o = resonant wavelength = 2370A° for tysonite

These expressions apply with good accuracy near resonance. At wavelengths removed from the resonance line, the absorption decreases faster than Eq. 2.30 indicates due to quantum considerations neglected in the derivation of the expression.

Evaluating $\frac{dn}{d\lambda}$ from Eq. 2.31 and using expressions 2.30, the ratio $(\frac{V}{a})$ appearing in Eq. 2.29 is:

$$\frac{V(\lambda)}{a(\lambda)} = (\frac{B}{2\pi G}) \quad \frac{\lambda^4 G^2 - \lambda_o^2(\lambda^2 - \lambda_o^2)^2}{\lambda^2 G^2 + (\lambda^2 - \lambda_o^2)^2} \tag{2.32}$$

for wavelengths within a few line-widths of resonance. Substituting $\lambda = \lambda_o + \delta G$, where δ is the deviation from resonance in line-widths, and neglecting δG with respect to λ_o reduces Eq. 2.32 to:

$$\frac{V}{a}(\delta) = \frac{B\lambda_o^2}{2\pi G} \left[\frac{1-4\delta^2}{1+4\delta^2}\right] \tag{2.33}$$

The largest value of this ratio occurs at resonance ($\delta=0$), for which

$$\frac{V}{a}(\lambda_o) = \frac{B\lambda_o^2}{2\pi G} \tag{2.34}$$

Equation 2.33 indicates that $(\frac{V}{a})$ also approaches $(-\frac{B\lambda_o^2}{2\pi G})$ for wavelengths many line widths removed from resonance. However, the actual attenuation decreases more rapidly away from resonance than Eq. 2.30 indicates, so that values of L necessary to satisfy Eq. 2.27 reach the limit of physically convenient crystal lengths. Under these conditions, the assumptions of Section E apply.

In the immediate vicinity of resonance (where the useful length of crystal is limited by resonant attenuation rather than by physical convenience) the largest value of $(\frac{V}{a})$ is given by Eq. 2.34. If a line width of $G=10A^o$ is assumed, and using $B=3\times10^{-4}$ radians per cm-oersted and $\lambda_o=2370A^o$ this maximum value of $(\frac{V}{a})$ is 2.7×10^{-7} radians per oersted. Using this value in Eq. 2.29

$$\frac{1}{H}\,\frac{i_s}{i_N} = 1.54\times10^{2}\,(I_1 R)^{1/2} \quad \text{per oersted} \tag{2.35}$$

In order to prevent saturating the photodetector with radiation outside the crystal resonance line, it is necessary that the line width of the source be no larger than the crystal absorption line width. Also to take advantage of the large Verdet constant at resonance, it is necessary that most of the source intensity be concentrated within about one quarter of the crystal line width either side of resonance (Eq. 2.33). For the assumed crystal line width of $10A^{o}$, the source intensity I_1 is that which could be produced by a source of line width about $5A^{o}$. Estimating this source intensity to be a maximum of about one watt, and using $R=5\times10^{-2}$ amperes per watt as a typical photodetector radiant sensitivity,[26] the estimated maximum current signal-to-noise ratio at the detector output for operation at optical resonance is

$$\left(\frac{1}{H}\,\frac{i_s}{i_N}\right)_{max} = 35 \text{ per oersted} \tag{2.36}$$

This analysis has assumed, in Eqs. 2.30, that the absorption and dispersion line widths were the same. If the absorption line width were appreciably narrower than the dispersion line width, the signal-to-noise ratio estimated in Eq. 2.36 would be increased.

E. ESTIMATE OF SIGNAL-TO-NOISE RATIO OFF RESONANCE

If the light source is operated at a wavelength several line widths away from resonance, the crystal attenuation becomes very small and the following assumptions can be made:

1. The maximum usable crystal length, L, is limited by physical size considerations rather than crystal attenuation;

2. The background intensity transmitted through the crystal and analyzer, in the absence of a magnetic field, is limited by the saturation level of the photodetector rather than by the available source intensity and the crystal attenuation.

A crystal length of 10 cm will be used in estimating signal-to-noise ratio. Reference 26 indicates that the cathode current $R I_b$ of the detector becomes a less-than-linear function of incident light intensity at a current of about 20 microamperes for typical photocathodes of about one inch diameter. Using these values for L and $R I_b$, Eq. 2.25 is

$$\frac{1}{H} \frac{i_s}{i_N} = 2.5 \times 10^7 \, V \frac{\sin 2\phi_o}{\tau_o + \sin^2 \phi_o} \tag{2.37}$$

The factor involving ϕ_o has a maximum value of $\left[\tau_o (1+\tau_o)\right]^{-1/2}$ at $\phi_o = \frac{1}{2} \cos^{-1}\left[\frac{1}{1+2\tau_o}\right]$ Provided $\tau_o \ll 1$, this maximum signal-to-noise ratio is

$$\frac{1}{H} \frac{i_s}{i_N} = 2.5 \times 10^7 \, (\tau_o)^{-1/2} \, V \tag{2.38}$$

Taking 4000 A^o as operating wavelength for this calculation, and using $V(4000\ A^o) = 1.4 \times 10^{-2}$ radians per cm-oersted at 4^oK (estimated in Appendix B), the signal-to-noise ratio is:

$$\frac{1}{H} \frac{i_s}{i_N} = 3.5 \times 10^5 \, (\tau_o)^{-1/2} \tag{2.39}$$

Assuming a polarizer transmission, τ_o, of 4×10^{-6} could be achieved, gives an estimated maximum signal-to-noise ratio for off-resonance operation:

$$\frac{1}{H} \frac{i_s}{i_N} = 1.75 \times 10^8 \text{ per oersted} \tag{2.40}$$

The magnetic field that produces a unity signal-to-noise ratio is

$$H(0 \text{ db}) = 6 \times 10^{-9} \text{ oersted} \tag{2.41}$$

Since the signal-to-noise ratio for off-resonance operation can be made larger than that for operation at resonance, the instrument should be operated at a source frequency well removed from crystal resonances, and the minimum detectable magnetic field strength is given by Eq. 2.41. This estimate of the smallest detectable field strength has used optimistic assumptions in evaluating the system parameters, and therefore represents a probable lower limit to the detectable magnetic field level. It should also be noted that the sensitivity estimated here applies only around a DC operating point of zero magnetic field. The detector would saturate if this operating point were changed appreciably due to stray fields.

CHAPTER III

USE OF THE MCIROWAVE FARADAY EFFECT TO MEASURE MAGNETIC FIELDS

A. INTRODUCTION

The direction of polarization of linearly polarized microwave energy is rotated in passing through a ferromagnetic dielectric in the presence of a DC magnetic bias field. This has been called the microwave Faraday effect from its similarity to the optical phenomenon discovered by Michael Faraday. The advent of low loss ferrimagnetic materials has made possible the construction of several types of microwave components using the Faraday effect mechanism to control the flow of microwave energy in a waveguide. Since the amount of rotation of the polarization vector through a ferrite is a function of the magnetic bias field, the phenomenon can also be used to measure magnetic field strength, and magnetometers using this principle have been constructed.[18] It is the purpose of the following sections to examine the factors influencing the sensitivity of such an instrument, and to estimate the smallest increment of magnetic field strength that such a device could be expected to detect under the most optimistic assumptions. This minimum detectable field can then be translated to angular rate threshold for a Faraday effect gyroscope by the methods of Chapter I.

B. MECHANISM OF MICROWAVE FARADAY EFFECT

The Faraday effect at microwave frequencies is caused by the interaction of the magnetic field of the propagating wave and the magnetic moments of electrons within the transmitting medium. The following description of the effect is adapted from a derivation by C. L. Hogan.[17]

A dipole of magnetic moment $\vec{u}_B$ in a magnetic field $\vec{H}$ feels a torque $\vec{u}_B \times \vec{H}$ which changes its angular momentum, $\vec{J}$, by $\vec{u}_B \times \vec{H} = \frac{d\vec{J}}{dt}$

If the magnetic moment of the dipole is caused by its angular momentum, and

is proportional to it by $\vec{u}_B = \gamma \vec{J}$, then the motion of the dipole in a magnetic field follows the relation, $\vec{u}_B \times \vec{H} = \frac{d\vec{J}}{dt} = \frac{1}{\gamma} \frac{d\vec{u}_B}{dt}$ If a unit volume of material contains $\underline{N}$ dipoles of moment $\vec{u}_B$, then its magnetization intensity is $\vec{M} = N \vec{u}_B$ when all the dipoles are aligned by an external field. For fields insufficient to saturate the material, the macroscopic magnetization vector $\vec{M}$ still follows the same equation as the microscopic dipoles:

$$\gamma \vec{M} \times \vec{H} = \frac{d\vec{M}}{dt} \tag{3.1}$$

Assume the magnetic field intensity and magnetization are constant in the z-component, and sinusoidal traveling waves in the x and y components:

$$\begin{aligned} H_z &= H_z \text{ (constant)} & M_z &= M_z \text{ (constant)} \\ H_x &= h_x e^{(j\omega t - \Gamma z)} & M_x &= m_x e^{(j\omega t - \Gamma z)} \\ H_y &= h_y e^{(j\omega t - \Gamma z)} & M_y &= m_y e^{(j\omega t - \Gamma z)} \end{aligned} \tag{3.2}$$

Then Eq. 3.1 for complex amplitudes is:

$$\begin{aligned} \gamma (m_y H_z - M_z h_y) &= j\omega m_x \\ \gamma (M_z h_x - m_x H_z) &= j\omega m_y \\ \gamma (m_x h_y - m_y h_x) e^{2(j\omega t - \Gamma z)} &= M_z \end{aligned} \tag{3.3}$$

The third equation gives $\dot{M}_z = 0$, provided $\frac{m_x}{h_x} = \frac{m_y}{h_y}$ Assuming this, and solving the remaining two equations for m_x and m_y:

$$m_x = - \frac{\gamma^2 H_z M_z h_x}{\omega^2 - \gamma^2 H_z^2} + j \frac{\omega \gamma M_z h_y}{\omega^2 - \gamma^2 H_z^2}$$

$$m_y = - \frac{\gamma^2 H_z M_z h_y}{\omega^2 - \gamma^2 H_z^2} - j \frac{\omega \gamma M_z h_x}{\omega^2 - \gamma^2 H_z^2} \qquad (3.4)$$

The flux density within the transmitting medium (cgs units) is:

$$b_x = h_x + 4\pi m_x$$

$$b_y = h_y + 4\pi m_y$$

where $\vec{B} = \begin{bmatrix} B_x \\ B_y \\ B_z \end{bmatrix}$ and $B_x = b_x e^{(j\omega t - \Gamma z)}$, $B_y = b_y e^{(j\omega t - \Gamma z)}$

Defining $\mu = 1 - \frac{\gamma^2 H_z M_z}{\omega^2 - \gamma^2 H_z^2}$

$$K = \frac{4\pi \omega \gamma M_z}{\omega^2 - \gamma^2 H_z^2} \qquad (3.5)$$

then $b_x = \mu h_x + j K h_y$

$$b_y = \mu h_y - j K h_x \qquad (3.6)$$

Maxwell's equations (cgs units) require that the magnetic field satisfy:

$$\nabla^2 \vec{H} = \frac{\epsilon}{c^2} \frac{\partial^2 \vec{B}}{\partial t^2}$$

Substituting expressions 3.6 into this equation gives (x and y components):

$$\nabla^2\left[h_x\, e^{(j\omega t - \Gamma z)}\right] = \frac{\epsilon}{c^2}\,(\mu\, h_x + j\, K\, h_y)\,\frac{\partial^2}{\partial t^2}\, e^{(j\omega t - \Gamma z)}$$

$$\nabla^2\left[h_y\, e^{(j\omega t - \Gamma z)}\right] = \frac{\epsilon}{c^2}\,(\mu\, h_y - j\, K\, h_x)\,\frac{\partial^2}{\partial t^2}\, e^{(j\omega t - \Gamma z)} \qquad (3.7)$$

Upon substitution into Eq. 3.7, it is found that the propagation constant, Γ, is different for positive and negative circularly polarized waves. For positive-rotating circularly polarized waves, $h_x = +j\, h_y$ and, taking the indicated partial derivatives in Eq. 3.7,

$$\Gamma^2(h_x\, e^{j\omega t - \Gamma z}) = -\omega^2\,(\frac{\epsilon}{c^2})\,(\mu + K)h_x\, e^{j\omega t - \Gamma z}$$

$$\Gamma^2(h_y\, e^{j\omega t - \Gamma z}) = -\omega^2\,(\frac{\epsilon}{c^2})\,(\mu + K)h_y\, e^{j\omega t - \Gamma z} \qquad (3.8)$$

or

$$\Gamma_+ = \frac{j\omega}{c}\left[\epsilon(\mu + K)\right]^{1/2}$$

Similarly for negative-rotating circularly polarized waves ($h_y = +\, j\, h_x$), the propagation constant is

$$\Gamma_- = \frac{j\omega}{c}\left[\epsilon(\mu - K)\right]^{1/2} \qquad (3.9)$$

Allowing for a complex dielectric constant $\epsilon = \epsilon' - j\epsilon''$, the attentuation and phase constants are:

$$\alpha_\pm = \mathrm{Re}\left[\Gamma_\pm\right] = \mathrm{Re}\left\{\frac{j\omega}{c}\left[(\epsilon' - j\epsilon'')(\mu \pm K)\right]^{1/2}\right\} \qquad (3.10)$$

$$\beta_\pm = \mathrm{Im}\left[\Gamma_\pm\right] = \mathrm{Im}\left\{\frac{j\omega}{c}\left[(\epsilon' - j\epsilon'')(\mu \pm K)\right]^{1/2}\right\} \qquad (3.11)$$

(Note K and μ are real, since no damping was assumed in Eq. 3.1.)

Taking real and imaginary parts of $\Gamma_{\pm}$:

$$\alpha_{\pm} = \frac{\omega}{c} (\mu \pm K)^{1/2} \left(\frac{|\epsilon''| - \epsilon'}{2}\right)^{1/2} \tag{3.12}$$

$$\beta_{\pm} = \frac{\omega}{c} (\mu \pm K)^{1/2} \left(\frac{|\epsilon| + \epsilon'}{2}\right)^{1/2} \tag{3.13}$$

A linearly polarized wave incident on the dielectric material can be regarded as splitting into positive and negative rotating circularly polarized components, which travel at different velocities according to Eq. 3.13. The superposition of the rotating waves after traveling a distance L yields a linearly polarized component whose polarization has rotated through an angle θ from its initial direction, given by

$$\theta = \frac{1}{2} \omega L \left(\frac{1}{V^+} - \frac{1}{V^-}\right) = \frac{1}{2} L (\beta_+ - \beta_-) \tag{3.14}$$

The principal effect of a low-loss ferrimagnetic dielectric upon a linearly polarized plane wave travelling through it, in the presence of a small DC magnetic field ($\gamma H_z \ll \omega$), thus, is to rotate the direction of polarization of the wave according to Eq. 3.14.

The propagation constants of Eqs. 3.8 and 3.9 were calculated for an unlimited expanse of dielectric. If instead the dielectric is contained within a waveguide of circular cross-section, a similar effect will occur with respect to the polarization direction of the field within the waveguide. Any propagating mode in a guide with a homogeneous, isotropic dielectric can be regarded as composed of several TEM waves travelling obliquely through the guide and rebounding from its walls, and creating an interference pattern that represents the actual measurable field distribution within the guide. The principal effect of filling the guide with an anisotropic ferrimagnetic material is the rotation of the polarization direction of these TEM component waves as they travel down the guide. Consequently the waveguide mode which results from the superposition of these component TEM waves

will have its polarization direction (s) rotated progressively as it travels through the guide. The dielectric attenuation and phase constants which apply to the actual waveguide mode and relate to distance measured along the guide axis can be obtained by multiplying the "unbounded" solution of Eqs. 3.12 and 3.13 by

$$\left[1 - \left(\frac{\omega_c}{\omega}\right)^2\right]^{1/2}$$

where ω_c is the cutoff angular frequency of the waveguide for the particular mode in question.[27] The resulting attenuation and phase constants are:

$$\alpha_{g\pm} = \frac{\omega}{c}(\mu \pm K)^{1/2}\left(\frac{|\epsilon| - \epsilon'}{2}\right)^{1/2}\left[1 - \left(\frac{\omega_c}{\omega}\right)^2\right]^{1/2} \qquad (3.15)$$

$$\beta_{g\pm} = \frac{\omega}{c}(\mu \pm K)^{1/2}\left(\frac{|\epsilon| + \epsilon'}{2}\right)^{1/2}\left[1 - \left(\frac{\omega_c}{\omega}\right)^2\right]^{1/2} \qquad (3.16)$$

The angle through which the direction of polarization of a particular waveguide mode is rotated over a length L of circular waveguide is obtained from Eqs. 3.16 and 3.14:

$$\theta_g = \frac{1}{2}\frac{L\omega}{c}\left(\frac{|\epsilon| + \epsilon'}{2}\right)^{1/2}\left[1 - \left(\frac{\omega_c}{\omega}\right)^2\right]^{1/2}\left[(\mu + K)^{1/2} - (\mu - K)^{1/2}\right] \qquad (3.17)$$

Substituting μ and K from Eq. 3.5

$$\theta_g = \frac{1}{2}\frac{L\omega}{c}\left(\frac{|\epsilon| + \epsilon'}{2}\right)^{1/2}\left[1 - \left(\frac{\omega_c}{\omega}\right)^2\right]^{1/2}\left[\left(1 - \frac{\gamma M_z(\gamma H_z - 4\pi\omega)}{\omega^2 - \gamma^2 H_z^2}\right)^{1/2} - \left(1 - \frac{\gamma M_z(\gamma H_z + 4\pi\omega)}{\omega^2 - \gamma^2 H_z^2}\right)^{1/2}\right] \qquad (3.18)$$

If the DC magnetic field is sufficiently small that γH_z can be neglected with respect to ω, then expression 3.18 simplifies to

$$\theta_g = \frac{1}{2}\,\frac{L\omega}{c}\left(\frac{|\epsilon|+\epsilon'}{2}\right)^{1/2}\left[1-\left(\frac{\omega_c}{\omega}\right)^2\right]^{1/2}\left[\left(1+\frac{4\pi\gamma M_z}{\omega}\right)^{1/2}-\left(1-\frac{4\pi\gamma M_z}{\omega}\right)^{1/2}\right] \tag{3.19}$$

Assuming that $\frac{4\pi\gamma M_z}{\omega} \ll 1$, the radicals can be approximated as $\left(1 \pm \frac{4\pi\gamma M_z}{\omega}\right)^{1/2} \approx 1 \pm \frac{2\pi\gamma M_z}{\omega}$. Making this approximation:

$$\theta_g = \frac{1}{2}\,\frac{L\omega}{c}\left(\frac{|\epsilon|+\epsilon'}{2}\right)^{1/2}\left[1-\left(\frac{\omega_c}{\omega}\right)^2\right]^{1/2}\left(\frac{4\pi\gamma M_z}{\omega}\right) \tag{3.20}$$

Substituting $4\pi M_z \approx \mu_{DC} H_z$ gives an effective Verdet constant, for a circular guide filled with ferrite, of

$$V_g = \frac{\theta_g}{LH_z} = \frac{\gamma\mu_{DC}}{2c}\left(\frac{|\epsilon|+\epsilon'}{2}\right)^{1/2}\left[1-\left(\frac{\omega_c}{\omega}\right)^2\right]^{1/2} \tag{3.21}$$

C. RESONANCE EFFECTS

The analysis of Section B uses the assumption $\gamma H_z \ll \omega$. As the magnetic field strength is increased, it is found that near resonance ($\gamma H_z \approx \omega$) the Faraday rotation increases rapidly and is strongly dependent on frequency. The dielectric attenuation also reaches a peak at resonance for positive circularly polarized waves, while negative circularly polarized waves are very little affected. Consequently if linearly polarized energy is transmitted into a ferrimagnetic medium with the external bias field adjusted to resonance for the carrier frequency, the energy leaving the medium is nearly all circularly polarized in the negative sense with a very small linearly polarized component. Under these conditions it is very difficult to measure the polarization direction of the linearly polarized component of the output.

Operating a microwave magnetometer at resonance also implies a bias field to produce ferromagnetic resonance at the carrier frequency chosen (e.g., $\approx$ 350 oersteds for 1 Kmc), in the absence of the small ΔH which it is desired to detect. A variation of either the bias field or carrier

frequency would cause an output indication; for example, a variation in carrier frequency of 0.03 cps corresponds to about 10^{-8} oersted ΔH. Because of the difficulty of maintaining a constant carrier frequency with microwave equipment, and the difficulty of measuring the polarization angle of the small linearly polarized component of the total energy leaving a ferrite rotator at resonance, it would seem the chances for detecting very small magnetic field increments are better at a low bias field, where $\omega >> \gamma H_z$ and the Faraday rotation is practically independent of carrier frequency.

D. SENSITIVITY OF MICROWAVE MAGNETOMETER

P. J. Allen[18] describes a device using the Faraday effect in ferrites at microwave frequencies to detect small changes in magnetic field. His device consisted of a short length of cylindrical waveguide with a thin pencil of ferrite at its center, and with pieces of rectangular guide coupled to each end with their orientations crossed. For a device of this type the electric field intensity coupled into the output section of rectangular waveguide is approximately

$$E_{out} = E_{in} \text{ (attenuation) } \left[t_o + \sin (V_g LH) \right] \qquad (3.22)$$

where the (attenuation) factor accounts for all losses between the input and output waveguide sections except the polarization mismatch at the output. The transmission through this mismatch of polarization, in the absence of a magnetic field H, is represented by the term t_o. The response of this device to small magnetic fields is indicated by its magnetic sensitivity, which will be defined as

$$\text{Sensitivity} = S = \frac{1}{E_{in}} \frac{dE_{out}}{dH} \qquad (3.23)$$

If the (attenuation) factor in Eq. 3.22 does not change with small changes in magnetic field, and if the total polarization rotations through the cylindrical guide section are small enough that $\cos (V_g LH) \approx 1$, then the magnetic sensitivity is approximately:

$$S = V_g L \text{ (attenuation)} \qquad (3.24)$$

J. H. Rowen[23] discusses several types of losses in ferrite devices. Those contributing significantly to the attenuation at very low fields are:

1. zero-field loss
2. normal dielectric loss
3. miscellaneous losses - e. g., waveguide wall attenuation, reflection, mode conversion

The normal dielectric loss is the only loss component that can be easily related to the material constants of the ferrite, in parameters commonly quoted by manufacturers. To develop the most optimistic estimate of the sensitivity of a microwave magnetometer, it might be supposed that a ferrite could be biased out of the region where the zero-field loss predominates by a constant bias field that was still not strong enough to produce ferromagnetic resonance and the accompanying carrier frequency sensitivity and resonance absorption. The third category of losses listed, "miscellaneous," is intended to include those determined by the precise choice of the configuration of the instrument, and for this optimistic estimate of magnetometer sensitivity they will be assumed to be zero. So the total loss, and consequently the attenuation constant, will be assumed to be derived solely from the normal dielectric loss. The attenuation constant is then given by Eq. 3. 15 of Section B:

$$\alpha_{g\pm} = \frac{\omega}{c} (\mu \pm K)^{1/2} \left(\frac{|\epsilon| - \epsilon'}{2}\right)^{1/2} \left[1-\left(\frac{\omega_c}{\omega}\right)^2\right]^{1/2} \qquad (3.25)$$

For very small values of H_z, $\mu \approx 1$ and $K \ll \mu$ (Eq. 3. 5) so the sensitivity is

$$S = \frac{V_g c}{\omega\left(\frac{|\epsilon| - \epsilon'}{2}\right)^{1/2}\left[1-\left(\frac{\omega_c}{\omega}\right)^2\right]^{1/2}} \frac{\omega L}{c}\left(\frac{|\epsilon| - \epsilon'}{2}\right)^{1/2}\left[1-\left(\frac{\omega_c}{\omega}\right)^2\right]^{1/2} \exp\left\{-\frac{\omega L}{c}\left(\frac{|\epsilon| - \epsilon'}{2}\right)^{1/2}\left[1-\left(\frac{\omega_c}{\omega}\right)^2\right]^{1/2}\right\} \qquad (3.26)$$

For a particular dielectric material and a specific carrier frequency, the greatest sensitivity can apparently be achieved by choosing the length L so that

$$\frac{\omega L}{c}\left(\frac{|\epsilon| - \epsilon'}{2}\right)^{1/2}\left[1-\left(\frac{\omega_c}{\omega}\right)^2\right]^{1/2} = 1 \qquad (3.27)$$

This condition for L may involve inconveniently long waveguide sections in the case of very low loss dielectrics. However, Eq. 3.27 will be used without regard to practical limitations on L in order to estimate the greatest possible sensitivity. In this case the maximum sensitivity for a given material and carrier frequency is

$$S_{max} = \frac{V_g c}{\omega e}\left(\frac{|\epsilon| - \epsilon'}{2}\right)^{-1/2}\left[1-\left(\frac{\omega_c}{\omega}\right)^2\right]^{-1/2} \qquad (3.28)$$

Substituting expression 3.21 for V_g:

$$S_{max} = \frac{\gamma \mu_{DC}}{2\omega e}\left(\frac{|\epsilon| + \epsilon'}{|\epsilon| - \epsilon'}\right)^{1/2} = \frac{\gamma \mu_{DC}}{2\omega e \tan\left(\frac{1}{2}\delta\right)} \qquad (3.29)$$

where δ is the loss angle of the dielectric, i.e., $\tan\delta = \frac{\epsilon''}{\epsilon'}$ If $\tan\delta \ll 1$, then Eq. 3.29 is approximately

$$S_{max} = \frac{\gamma \mu_{DC}}{\omega e \tan\delta} \qquad (3.30)$$

If a ferrite with a ratio of $\frac{\mu_{DC}}{\tan\delta} = 10^4$ at one kilomegacycle could be obtained, then using $\gamma = 1.76\times10^7$, the estimated maximum sensitivity is $S_{max}=10$ per oersted. This is felt certainly to be an optimistic estimate, due to the losses neglected and the inconveniently long ferrite loaded guide implied by Eq. 3.27 for low-loss dielectrics.

P. J. Allen[18] found that magnetic field increments of the order of 10^{-5} oersteds could be detected with an X-band microwave device of magnetic sensitivity S=0.04 per oersted. Assuming that the minimum detectable field increment is inversely proportional to magnetic sensitivity (discussed in Appendix D), the estimated maximum sensitivity of 10 per oersted implies a minimum detectable field increment of

$$\Delta H_{min} = 4 \times 10^{-8} \text{ oersted} \qquad (3.31)$$

CHAPTER IV

TRANSIT-TIME EFFECTS

A. TRANSIT-TIME EFFECTS IN ISOTROPIC MEDIA

Consider the system shown in Fig. 2. Light is sent parallel to the axis of the system--in the z direction--and if the polarizer and analyzer are crossed, no light reaches the photodetector. If, however, we cause the system to rotate about the z-axis with an angular velocity Ω some light can get through. Suppose, for example, the polarizer is

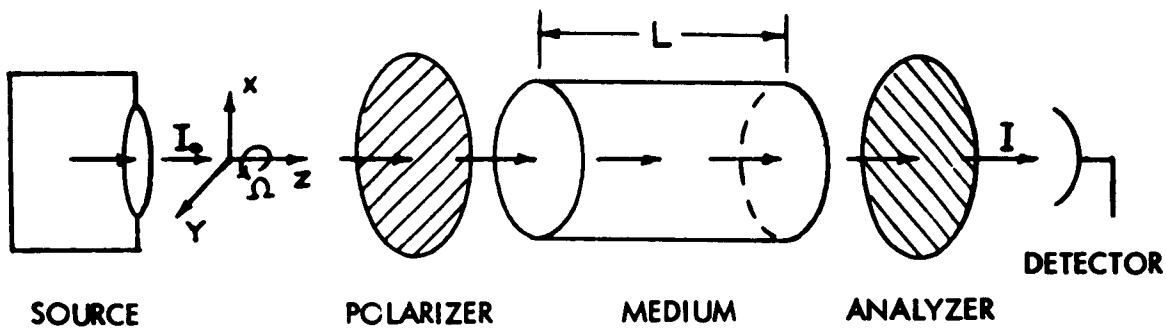

Fig. 2 Transit-Time Method

set to pass light polarized in the x-direction at time t=0. At this time the analyzer can pass only light polarized in the y-direction. In the time $t=\frac{L}{C}$ that it takes for the light to reach it the analyzer has rotated by the angle $\theta = \frac{\Omega L}{C}$ radians. C is the speed of light if we assume the "medium" is vacuum and L is the length of the light path through the medium. If I_o is the intensity of the unpolarized incident light, the intensity I of light that reaches the photodetector is given by

$$I = \frac{1}{2} I_o \sin^2 \theta \approx \frac{1}{2} I_o \left(\frac{\Omega L}{C}\right)^2 \qquad (4.1)$$

for perfect polarizers. For L=1 meter, $\frac{\Omega}{2\pi} = 1$ revolution per sec, $\frac{I}{I_o} = 4.4 \times 10^{-16}$. The best polarizers have a minimum transmission of the order of 10^{-6}, that is 100 db larger than the effect at 1 revolution per second.

The transmission through the system could be enhanced by putting the polarizers outside of a Fabry-Perot interferometer. Assuming a maximum reflection coefficient at the Fabry Perot plate of 99.5 percent, we can expect, at an angular rate of 1 revolution per second, a transmission of $\frac{I}{I_o} = 4.4 \times 10^{-14}$ against a zero-signal background of $2.5 \times 10^{-9} I_o$. Our experience indicates that it is practically impossible to detect a signal which is of the order of 50 db weaker than the background intensity. Further study of the photodetector noise problem, similar to that conducted for the optical Faraday effect, indicates that, for a source intensity adjusted to give optimum detector current, the minimum detectable angular rate is 130 radians per second. Note that this sensitivity has been estimated for a path length of 1 meter whereas the Faraday effect calculations have assumed a path length of 0.10 meter. Thus the resolution of a device that depends solely upon the transit time effect for creating a rotation of the plane of polarization is of the order of 10,000 times smaller than one that employs the Faraday effect in addition to transit time effects.

B. TRANSIT TIME EFFECTS IN ANISOTROPIC MEDIA

Consider now that we replace the isotropic medium considered above by one that has a dielectric tensor

$$\epsilon = \begin{bmatrix} \epsilon_x & 0 & 0 \\ 0 & \epsilon_y & 0 \\ 0 & 0 & \epsilon_y \end{bmatrix} \quad \epsilon_x \neq \epsilon_y \qquad (4.2)$$

What is the effect of rotation on the light transmitted by this system. The coordinate system in Fig. 3 will be convenient.

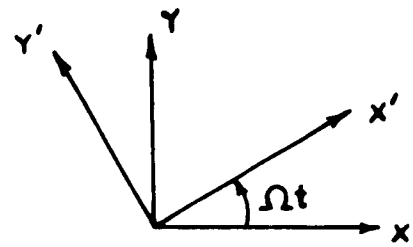

Fig. 3 Coordinate System

In tensor notation

$$\begin{bmatrix} x \\ y \end{bmatrix} = R \begin{bmatrix} x' \\ y' \end{bmatrix} \quad : \quad R = \begin{bmatrix} \cos\Omega t & -\sin\Omega t \\ \sin\Omega t & \cos\Omega t \end{bmatrix} \tag{4.3}$$

With a proper choice of units one can write two of Maxwell's equations for a non-conducting medium as follows

$$\begin{aligned} \nabla \times E &= -\dot{H} \\ \nabla \times H &= \dot{D} \end{aligned} \tag{4.4}$$

For plane waves propagating in the z direction

$$\partial_{zz} E = \ddot{D} \; ; \quad E = \begin{bmatrix} E_x \\ E_y \end{bmatrix} , \; D = \begin{bmatrix} D_x \\ D_y \end{bmatrix} = \begin{bmatrix} \epsilon_{xx} & \epsilon_{xy} \\ \epsilon_{yx} & \epsilon_{yy} \end{bmatrix} \begin{bmatrix} E_x \\ E_y \end{bmatrix} \tag{4.5}$$

$$\begin{bmatrix} \epsilon_{xx} & \epsilon_{xy} \\ \epsilon_{yx} & \epsilon_{yy} \end{bmatrix} = R \begin{bmatrix} \epsilon'_x & 0 \\ 0 & \epsilon'_y \end{bmatrix} R^{-1} \tag{4.6}$$

The medium rotates with the (x' y') system. One can then show

$$\partial_{zz} E'_x = \epsilon'_x \left(\partial_{tt} E'_x - \Omega^2 E_{x'} \right) - 2\Omega \epsilon'_y \dot{E}_{y'}$$

$$\partial_{yy} E'_y = \epsilon'_y \left(\partial_{tt} E'_y - \Omega^2 E_{y'} \right) + 2\Omega \epsilon'_x \dot{E}_{x'} \qquad (4.7)$$

With our choice of units we can use for trial solutions

$$\begin{bmatrix} E'_x \\ E'_y \end{bmatrix} = \begin{bmatrix} A \\ B \end{bmatrix} e^{(t-kz)} \qquad (4.8)$$

Putting this into Eq. 4.7 and solving for k

$$k_{\pm}^2 = \frac{1+\Omega^2}{2} (\epsilon'_x + \epsilon'_y) \pm \frac{1+\Omega^2}{2} (\epsilon'_x - \epsilon'_y) \left[1 + \frac{16\Omega^2 \epsilon'_x \epsilon'_y}{(1+\Omega^2)^2 (\epsilon'_x - \epsilon'_y)^2} \right]^{1/2} \qquad (4.9)$$

Assuming $\Omega \ll \epsilon'_x - \epsilon'_y$, the difference in propagation constants for the two modes is

$$k_+ - k_- \approx \left[\frac{1+\Omega^2}{2} \right]^{1/2} \frac{(\epsilon'_x - \epsilon'_y)}{\sqrt{\epsilon'_x + \epsilon'_y}} \left[1 + \frac{8\Omega^2 \epsilon'_x \epsilon'_y}{(\epsilon'_x - \epsilon'_y)^2} \right] \qquad (4.10)$$

The relative amplitude of the modes are,

$$\left(\frac{B}{A}\right)_{\pm} = \frac{\left(\frac{1+\Omega^2}{2}\right)(\epsilon'_y - \epsilon'_x)}{2i\Omega\epsilon'_y} \left[1 \mp 1 \mp \frac{8\Omega^2 \epsilon'_x \epsilon'_y}{(\epsilon'_x - \epsilon'_y)^2} \right] \qquad (4.11)$$

For $\Omega << 1$

$$\frac{B_+}{A_+} = - \frac{i2\Omega\epsilon'_x}{\epsilon'_x - \epsilon'_y} \quad ; \quad \frac{A_-}{B_-} = - \frac{2i\Omega\epsilon'_y}{\epsilon'_x - \epsilon'_y} \tag{4.12}$$

The two modes are

$$E_+ = A_+ \begin{bmatrix} 1 \\ \\ \dfrac{-i2\Omega\epsilon'_x}{\epsilon'_x - \epsilon'_y} \end{bmatrix} e^{(t-k_+z)}$$

$$E_- = B_- \begin{bmatrix} \dfrac{-i2\Omega\epsilon'_y}{\epsilon'_x - \epsilon'_y} \\ \\ 1 \end{bmatrix} e^{(t-k_-z)} \tag{4.13}$$

If the polarizer can pass only light polarized in the x' - direction

$$E = E_o \left\{ \begin{bmatrix} 1 \\ \\ \dfrac{-i2\Omega\epsilon'_x}{\epsilon'_x - \epsilon'_y} \end{bmatrix} e^{(t-k_+z)} + \frac{i2\Omega\epsilon'_x}{\epsilon'_x - \epsilon'_y} \begin{bmatrix} \dfrac{i2\Omega\epsilon'_y}{\epsilon'_x - \epsilon'_y} \\ \\ 1 \end{bmatrix} e^{(t-h_-z)} \right\} \tag{4.14}$$

After a length L of crystal the analyzer will pass only the y' - component of E. Using Eq. 4.10 for $\frac{(k_+ - k_-)}{2} L << 1$

$$|E_{y'}| = \frac{4\Omega\epsilon'_x}{\epsilon'_x - \epsilon'_y} \sin\left(\frac{k_+ - k_-}{2}\right) L \approx \frac{4\Omega\epsilon'_x L}{\left[2(\epsilon'_x + \epsilon'_y)\right]^{1/2}} \qquad (4.15)$$

Or the transmission coefficient for intensity is

$$\frac{I}{I_o} = \Omega^2 \frac{\epsilon_{x'}^2}{\epsilon'_x + \epsilon'_y} L^2 \qquad (4.16)$$

To convert to conventional units we replace L by $\frac{2\pi L}{\lambda_o}$ and Ω by $\frac{\Omega}{2\pi C}\lambda_o$. Then for $\epsilon'_x \approx \epsilon'_y = \bar{\epsilon}$

$$\frac{I}{I_o} = \frac{1}{2}\left(\frac{L\Omega}{C}\right)^2 \bar{\epsilon} \qquad (4.17)$$

Compare Eqs. 4.17 and 4.1. For the case $\bar{\epsilon} = 1$ they are identical. If we note that the effective length of a dielectric is $\sqrt{\epsilon}\ L$ we see Eq. 4.17 is consistent with physical reasoning.

For the same reasons as for $\bar{\epsilon} = 1$ we do not get an appreciable effect for $\frac{\Omega}{2\pi} \sim 1$ revolution per second, a length of 1 meter, and $\epsilon \approx 10$ (which is larger than most real solids).

The only remaining unanswered point in this approach is to consider the possibility of the approximation $\frac{\Omega}{2C}\lambda_o \ll \epsilon'_x - \epsilon'_y$ not being correct. Note that $\lambda_o/C \sim 10^{-15}$ seconds so $\frac{\Omega}{2\pi} \sim 1$ makes $\epsilon'_x - \epsilon'_y \gg 10^{-15}$ the requirement. This inequality is satisfied for all real crystals that we call anisotropic. If $\epsilon'_x - \epsilon'_y \lesssim 10^{-15}$ the crystal behaves isotropically.

We thus conclude two things:

1. The time of flight for light between two points of the order a meter away from one another is too short to be used to measure angular rotation, if detection is based on changes in angle of polarization. This conclusion holds even if multiple reflections are used.
2. The screw symmetry, similar to the transformation properties of a magnetic field, that must be linear in $\epsilon'_x - \epsilon'_y$ is at least quadratic in Ω, i.e. Eq. 4.15 carried out to Ω^2 will show this effect, and much weaker than the simple effect we have just seen.

APPENDIX A

MAGNITUDE OF FARADAY ROTATION IN DIFFERENT TYPES OF MATERIALS

1. GASES

The following table of Verdet constants for some common gases is from Reference 1. Values were measured at 17°C and 5780A°, and reduced to one atmosphere pressure.

Gas	V (microminutes per cm-gauss)	Gas	V
He	0.474	NH_3	19.20
Kr	18.60	CH_3CH_3	24.51
Xe	43.59	$CH_3(CH_2)_2CH_3$	45.17
NO	69.49	Freon-12	32.86

2. LIQUIDS

Some Verdet constants for liquids are listed below.

Liquid	Temp.	V(milli-minutes per cm-gauss)	Wavelength	Reference
HNO_3	16°C	8.76	5893A°	2
CH_3CH_2OH	25	11.12	5893	2
$C Cl_4$	17	16.90	5780	1

Verdet constants for aqueous solutions, at 23°C. Data are from Reference 2, Verdet constant in milli-minutes per cm-gauss.

Solute	6000A°	8000A°	10,000A°	12,500A°	Concentration
pure H_2O	12.6	7.0	4.4	2.9	----------
$Ce(NO_3)_3$	6.2	3.9	2.4	1.6	1.2 gm per cc.
$Fe_2 Cl_6$	10.7	6.1	4.0	2.6	1.049
$Fe_2 Cl_6$	---	39.9	27.5	11.0	1.523

The ratio of Verdet constants for liquid and vapor phase of some materials are listed below from Reference 1. They were measured in the range 50°C to 70°C, and at wavelength 5780A°.

Substance	Ratio of Verdet Constants	Ratio of Densities
H_2O	1239	------
CH_3CH_2OH	443	471
CH_3OH	645	658
$C Cl_4$	287	------

3. SOLIDS

a. Non-Ferrous, without Free Carriers

Typical Verdet constants of non-magnetic solids are listed below, from Reference 3. Temperatures 16°C to 19°C, wavelength 5893A°.

Material	V (milli-minutes per cm-oersted)
Amber	9.60
NaCl	35.85
Glass (various kinds)	15 to 100
ZnS	225
CaF_2	8.83

Some crystals containing rare earth ions have particularly large saturation magnetizations, and correspondingly large Faraday rotations. The Faraday rotations listed below are near saturation values.

Material	Temp	H	λ	Faraday Rotation	Ref.
Tysonite	1.95°K	26.7 K-Oer.	4743A°	17,410°/mm	6
Parisite	4.21	26.7	5650	3692	6
Bastnaesite	4.21	26.7	5650	4268	6
Xenotime	1.38	26.5	5616	940	5
$Ce(PO_3)_3$	1.8	70	5461	8570	7
$Dy(SO_4C_2H_5)_39H_2O$	1.6	26.9	5770	593	4
$Er(SO_4C_2H_5)_39H_2O$	1.4°K	27.2 K-Oer.	5770A°	126°/mm	4
$Pr(SO_4C_2H_5)_39H_2O$	1.45	26.9	5770	485	4
$Nd(SO_4C_2H_5)_39H_2O$	1.48	27.2	5770	1146	4
$Ce(SO_4C_2H_5)_39H_2O$	1.37	27.0	5770	4196	4

b. Semiconductors

Material	Carrier Concentration	Largest Observed V	λ	Ref
Germanium	Intrinsic	0.0023°/cm-gauss	2.5μ	8
n-Germanium	1.47×10^{17} per cm^3	0.0050	13μ	8
InSb	Intrinsic	*0.0010	8μ	28
n-InSb	1.8×10^{15} per cm^3	*0.016	20μ	28
n-InSb	6.5×10^{15}	*0.023	20μ	28
n-InSb	2.9×10^{16}	*0.049	19μ	28

Values marked with an (*) are given in Reference 28 as nV, where n is the index of refraction, so they must be divided by n to obtain the actual Verdet constant. From the data in Reference 9 it is estimated that n is less than 2 or 3 in each case.

c. Ferrimagnets

The following table of properties of yttrium-iron garnet is from Reference 10.

Wavelength	Attenuation	Faraday Rotation	Field Intensity
7700A°	1740 db/cm	800°/cm	2500 oersteds
6060	6090	2000	2500
5260	11, 300	4000	2500

No measurable transmission at higher frequencies was observed for crystal thicknesses 0.0025 cm. Total rotations measured were in the range 5 to 10 degrees.

Reference 11 lists the Faraday rotations observed with red light (around 7000A° or redder) in the following materials:

Material	Farady Rotation	Thickness
$Li_{0.5}Fe_{2.5}O_4$	1000 degrees/cm	0.005 inch
$MgFe_2O_4$	1100	0.008
$PbFe_{11}AlO_{14}$	4500	not recorded
$YFeO_3$	500	not recorded

The thicknesses recorded for $Li_{0.5}Fe_{2.5}O_4$ and $MgFe_2O_4$ are the greatest for which the crystals were transparent in the visible red light range. An arc lamp was used.

d. Ferromagnets

Reference 12 describes the use of the Faraday effect to detect domain boundaries within a 500A° film of 80 percent nickel and 20 percent iron. The domains were magnetized in the plane of the film, and it was necessary for light to pass obliquely through the film to observe the domain outlines. With a 45° angle of illumination, a Faraday rotation of nine minutes was observed upon completely reversing the magnetization of the film.

Reference 13 describes a 1000A° film of MnBi, which can be magnetized perpendicular to the plane of the film and produces a differential rotation of 10° when its magnetization is totally reversed. An external field of 3000 oersteds is necessary to saturate the film from its unmagnetized state.

APPENDIX B

ESTIMATE OF OPTICAL CONSTANTS FOR TYSONITE

Reference 22 gives an empirical formula for the Verdet constant for tysonite as:

$$V = \frac{C}{T+\theta} + B, \text{ where for green mercury light } (5461A^{\circ}):$$

C = -0.14209 degrees per mm-oersted-degree K

B = -0.0004514 degrees per mm-oersted

θ = 0.2942 degrees K

T = temperature in degrees K (B.1)

At $T = 4^{\circ}K$, formula B.1 gives

$V(5461A^{\circ})$ = 0.033 degrees per mm-oersted, or

$V(5461A^{\circ}) = 6 \times 10^{-3}$ radians per cm-oersted (B.2)

Measurements of the saturation rotation in tysonite at different wavelengths given in Reference 5 can be used to estimate the ratio of the Verdet constants at $4000A^{\circ}$ and $5461A^{\circ}$. Linearly interpolating this data gives a ratio of the saturation Faraday rotation in tysonite at $4000A^{\circ}$ to that at $5461A^{\circ}$ as 2.36. Assuming that the Verdet constants at these wavelengths are in the same ratio, the Verdet constant at $4000A^{\circ}$ would be:

$$V(4000A^{\circ}) = 1.4 \times 10^{-2} \text{ radians per cm-oersted at } 4^{\circ}K$$

APPENDIX C

PROPERTIES OF TYPICAL FERRITES

The following table of properties of varieties of Ferroxcube III (Mn - Zn ferrite) and IV (Ni - Zn ferrite) is from Reference 24:

Ferroxcube Type	Relative Initial Permeability	Freq. (KC) at which $\tan\delta = 0.1$	DC Resistivity (ohm - meters)	DC Relative Dielectric Constant
IIIA	1750	300 KC	1.8	$\approx 10^5$
IIIB	1245	460	1.5	
IIIC	1280	420	0.6	
IIID	806	830	1.0	
IVA	650	1500	$> 4 \times 10^4$	$\approx 10^3$
IVB	230	5500		
IVC	90	16,000		
IVD	45	29,000		
IVE	17	60,000		

The following table represents results of attempts to measure small fields by means of a microwave magnetometer as described in Reference 18. Data was taken at carrier frequency 9300mc.

"Ferramic" type	Rod Length	Rod Diam.	Total Xmission loss	$e^{-\alpha l}$	α (nepers/cm)	Sensitivity per oersted	V_g deg/cm-oer
D	1 5/8"	0.25	5 db	0.562	0.14	0.008	-0.2
D	4 7/8"	0.25	16.5db	0.147	0.14	0.040	1.3
A	1 5/8"	0.25	1.1db	0.881	0.032	0.003	0.05
A	4 7/8"	0.25	3.6db	0.661	0.032	0.025	0.2

APPENDIX D

RELATION OF MINIMUM DETECTABLE FIELD TO MAGNETIC SENSITIVITY

It is estimated in Section D of Chapter III that the electric field intensity coupled into the detector of a microwave Faraday effect magnetometer is a linear function of magnetic field intensity for small values of magnetic field. Specifically the output electric field is

$$E_{out} = E_{in} \text{ (attenuation) } (t_o + S\ \Delta H) \qquad \text{(D. 1)}$$

Assuming that the detector responds linearly to its input power, or to the square of expression D. 1, then the detector output indication is:

$$D = K\left[t_o^2 + 2t_o\ S\ \Delta H + S^2(\Delta H)^2\right] + \text{(noise)} \qquad \text{(D. 2)}$$

Here D is the detector output indication, and the term (noise) represents all noise generated within the detector. The carrier power level, attenuation through the waveguide and the detector gain have been absorbed into the constant K.

To determine whether the detector output bears essentially a linear or a quadratic relation to $S\ \Delta H$, it is necessary to examine the relative magnitudes of the terms in Eq. D. 2. The largest attenuation currently available from typical ferrite isolators is around 40 db. This indicates that the zero-signal transmission t_o would be probably at least 10^{-2}. Consequently the term that is linear in $S\ \Delta H$ in Eq. D. 2 dominates the quadratic term for values of $S\ \Delta H$ up to around 10^{-2}. Reference 18 indicates that an $S\ \Delta H$ of around 4×10^{-7} was detectable in the presence of the detector noise. Since this is well below the level where the term $S^2(\Delta H)^2$ in Eq. D. 2 becomes important, the detector signal output must have been a linear function of $S\ \Delta H$.

It seems most likely that for small magnetic fields (near the system noise level) the detector signal output in any practical Faraday effect magnetometer would be a linear function of $S\ \Delta H$, and for a given detector noise level the smallest detectable magnetic field increment is therefore inversely proportional to the magnetic sensitivity, S.

APPENDIX E

INFLUENCE OF POLARIZER AND ANALYZER ON OPTICAL SENSITIVITY

In Chapter II, Section C the transmission through a polarizer and analyzer, displaced from null by an angle θ, was assumed to be

$$\frac{I_0}{I_1} = \frac{1}{2} (\sin^2\theta + \tau_0) \qquad (E.1)$$

where I_1 is the incident (randomly polarized) light intensity, I_0 is the output light intensity, and τ_0 is the "leakage," a characteristic of the particular polarizer and analyzer used. The signal to noise ratio for a measurement of the angle θ by means of a photoemissive detector, computed in Chapter II, Section E, turns out to be a function of τ_0. Consequently it is desirable to examine in more detail the characteristics the polarizer and analyzer at small angles θ where the transmission τ_0 becomes important.

It was assumed in Chapter II that the light source was randomly polarized. Denoting the RMS value of the magnitude of the electric field intensity of the source as E_1, then the (RMS) components along the directions of maximum and minimum transmission of the polarizer are

$$\vec{E_1} = \begin{pmatrix} \text{RMS component parallel to polarizer axis} \\ \text{RMS component perpendicular to polarizer axis} \end{pmatrix} = \frac{E_1}{\sqrt{2}} \begin{pmatrix} 1 \\ 1 \end{pmatrix} \qquad (E.2)$$

Neglecting attenuation of the polarizer for incident waves polarized parallel to its axis, the transmission of the polarizer is

$$T_p = \begin{pmatrix} 1 & 0 \\ 1 & e_p \end{pmatrix} \qquad \text{(E.3)}$$

where e_p is the ellipticity of the polarizer.

If the analyzer is rotated by an angle $\theta_0 + \theta$ from its null orientation with the polarizer, then the transmission through the analyzer is

$$T_a = \begin{pmatrix} -\sin(\theta_0+\theta) & \cos(\theta_0+\theta) \\ e_a\cos(\theta_0+\theta) & e_a\sin(\theta_0+\theta) \end{pmatrix} \qquad \text{(E.4)}$$

In the expression above, e_a is the analyzer ellipticity and the incident wave is assumed to be resolved into components parallel and perpendicular to the axis of the polarizer, while the output wave is resolved into components parallel and perpendicular to the analyzer axis.

Ignoring any attenuation or coupling between orthogonally polarized modes, which might occur in the transmission medium a between polarizer and analyzer and assuming no reflection losses at interfaces between polarizer and analyzer, the electric field intensity reaching the detector $\vec{E}_0$ is given by the product of expressions E.2, E.3 and E.4:

$$\vec{E}_0 = \begin{pmatrix} -\sin(\theta_0+\theta) & \cos(\theta_0+\theta) \\ e_a\cos(\theta_0+\theta) & e_a\sin(\theta_0+\theta) \end{pmatrix} \begin{pmatrix} 1 & 0 \\ 0 & e_p \end{pmatrix} \frac{E_1}{\sqrt{2}} \begin{pmatrix} 1 \\ 1 \end{pmatrix} \qquad \text{(E.5)}$$

Performing the indicated multiplications of Eq. E.5, the output electric field intensity is

$$\vec{E}_0 = \frac{E_1}{2} \begin{pmatrix} e_p\cos(\theta_0+\theta)-\sin(\theta_0+\theta) \\ e_a\cos(\theta_0+\theta)+ e_a e_p\sin(\theta_0+\theta) \end{pmatrix} \qquad (E.6)$$

Denoting the RMS value of the electric field intensity at the detector as E_0, and neglecting higher powers of e's, the ratio of output light intensity I_0 to source intensity I_1 is

$$\frac{I_0}{I_1} = \frac{E_0^2}{E_1^2} = \frac{1}{2}\left\{(e_p^2+e_a^2)\cos^2(\theta_0+\theta)+\sin^2(\theta_0+\theta)- e_p\sin^2(\theta_0+\theta)\right\} \qquad (E.7)$$

This expression is equivalent to Eq. E.1, if $e_p = 0$ and if τ_0 is identified with e_a^2. The use of expression E.1 in Chapter II consequently corresponds to the assumption of a perfectly polarized source and an analyzer ellipticity of $e_a = \sqrt{\tau_0}$.

It was assumed in Chapter II that the threshold for detecting small derivations from zero in θ, by means of a photoemissive detector measuring I_0, would be limited by shot noise in the photodetector. Under these conditions the best signal to (shot) noise ratio per unit of θ at the detector output was found to occur with the bias angle θ_0 chosen according to

$$\cos 2\theta_0 = \frac{1}{1+2\tau_0} \qquad (E.8)$$

Under this condition, and again assuming the source is perfectly polarized, the ratio of detector light intensity to source intensity at zero signal is approximately τ_0 or e_a^2. It was assumed in Chapter II that the source intensity would be sufficient to saturate a photocathode of one inch diameter. This would require a detector light intensity of about 4×10^{-4} watts. Since a value of 4×10^{-6} was assumed for e_a^2, the source intensity required would be 100 watts exclusive of power lost (absorbed, reflected or scattered) previous to reaching the analyzer.

APPENDIX F

USE OF MIRRORS TO INCREASE OPTICAL PATH

The minimum detectable angular rate for a gyroscopic instrument based on the optical Faraday effect discussed in Chapter II or the transit-time effect of Chapter IV decreases as the active length of the optical path is increased, and it was necessary to assume a certain maximum practical length of the light path in order to estimate the minimum detectable angular rate. The optical pathlengths assumed were 10 cm. for the Faraday effect device and one meter for the transit time device. This length may be limited in practice by either the allowable physical size of the instrument or by the absorption. The effective length of the optical path can be increased without increasing the size of the instrument by the use of mirrors placed at the ends of the transmission path, at the cost of reducing the transmitted light intensity. Such an arrangement is shown in Fig. 4. The performance of such an arrangement will be examined here to determine if it offers possible improvement over the single pass system.

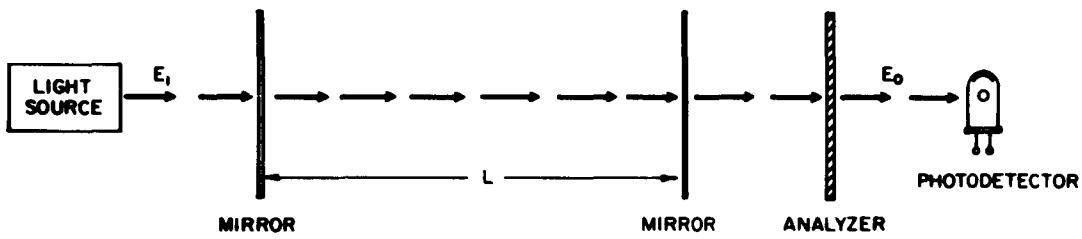

Figure 4

The light source will be assumed to produce a perfectly polarized beam, of electric field intersity E_1. The mirrors on either end of the active optical path have an electric field reflection coefficient of K or a power reflection coefficient of K^2. Neglecting scattering and absorption losses, and using expression E-4 for the analyzer transmission, the

components of electric field intensity E_o, referred to the analyzer axes, which reach the detector after 2n reflections are:

$$\vec{E}_o(n) = (1-K)^2 K^{2n} \begin{pmatrix} -\sin[\theta_o+(2n+1)\theta] & \cos[\theta_o+(2n+1)\theta] \\ e_a \cos[\theta_o+(2n+1)\theta] & e_a \sin[\theta_o+(2n+1)\theta] \end{pmatrix} \begin{pmatrix} E_1 \\ 0 \end{pmatrix} \tag{F-1}$$

Representing the component of E_o along the analyzer axis as Eo_1, and the perpendicular component as Eo_2, Eq. F-1 gives:

$$\left.\begin{aligned} Eo_1 &= -E_1 (1-K)^2 K^{2n} \sin[\theta_o+(2n+1)\theta] \\ Eo_2 &= E_1 (1-K)^2 K^{2n} e_a \cos[\theta_o+(2n+1)\theta] \end{aligned}\right\} \tag{F-2}$$

The photodetector indicated in Fig. F-1 would produce a current proportional to the light intensity, or to E_o^2. In evaluating the intensity, it is necessary to consider both coherent and incoherent sources. In the case of an incoherent source, the intensity at the photodetector is proportional to

$$I_o \sim \sum_{n=o}^{\infty} [Eo_1^2(n) + Eo_2^2(n)] \tag{F-3}$$

and in the case of a coherent and monochromatic source of proper frequency so that the distance L is a whole number of half wavelengths, the intensity at the detector is proportional to

$$I_o \sim \left[\sum_{n=o}^{\infty} Eo_1(n)\right]^2 + \left[\sum_{n=o}^{\infty} Eo_2(n)\right]^2 \tag{F-4}$$

The ratio of detector intensity to source intensity, for an incoherent source, is

$$\frac{I_o}{I_1} = \frac{1}{2}(1-K)^2 \left\{ \frac{1+e_a^2}{1-K^4} \right.$$

$$\left. - (1-e_a^2) \frac{\cos 2(\theta_o+\theta) - K^4 \cos 2(\theta_o-\theta)}{1+K^8 - 2K^4 \cos 4\theta} \right\} \qquad \text{(F-5)}$$

where I_1 is the source intensity. For a coherent monochromatic source of proper wavelength, the intensity at the detector is

$$\frac{I_o}{I_1} = (1-K)^4 \left\{ \frac{-\sin(\theta_o+\theta)+K^2\sin(\theta_o-\theta)}{(1+K^4) - 2K^2\cos 2\theta} \right\}^2$$

$$+ e_a^2 (1-K)^4 \left\{ \frac{\cos(\theta_o+\theta) - K^2\cos(\theta_o-\theta)}{(1+K^4) - 2K^2\cos 2\theta)} \right\}^2 \qquad \text{(F-6)}$$

The background light intensity, I_b, reaching the detector in the absence of a signal (θ=o) is, for the incoherent source,

$$\frac{I_b}{I_1} = \frac{1}{2} \frac{(1-K)^4}{(1-K^4)} \left[1+e_a^2 - (1-e_a^2)\cos 2\theta_o \right] \qquad \text{(F-7)}$$

For the coherent, monochromatic case, it is

$$\frac{I_b}{I_1} = \frac{(1-K)^2}{(1+K)^2} \left(\sin^2\theta_o + e_a^2 \cos^2\theta_o \right) \qquad \text{(F-8)}$$

Equations F-7 and F-8 indicate that the background transmission in either the coherent or incoherent case is reduced from the corresponding transmission evaluated in Appendix E for the case without mirrors, provided that the value of θ_o chosen is of about the same order of magnitude with and without mirrors. Since it was found in Appendix E that an input power of about 100 watts plus losses was required before a detector of typical size would

saturate, then for sources of moderate power level, detector saturation should not be a problem when mirrors are used, in either the coherent or incoherent case. For this reason, the detector current signal to noise ratio will be evaluated assuming I_1 constant at its highest practical power level, and the parameters θ_o and K will be chosen to give the best output signal to noise ratio under this condition. This assumption will be reconsidered when the use of pulsed sources is discussed in Appendix G.

With a detector of radiant sensitivity R, the RMS shot noise current in a bandwidth Δf for the incoherent case is

$$i_n = \left(\frac{e \Delta f R I_1}{1-K^4}\right)^{\frac{1}{2}} (1-K)^2 \left[1+e_a^2 - (1-e_a^2)\cos 2\theta_o\right]^{\frac{1}{2}} \qquad \text{(F-9)}$$

For the coherent case, the RMs shot noise current is

$$i_n = (2e \Delta f R I_1)^{\frac{1}{2}} \left(\frac{1-K}{1+K}\right) (\sin^2 \theta_o + e_a^2 \cos^2 \theta_o)^{\frac{1}{2}} \qquad \text{(F-10)}$$

The "signal" current per unit θ is

$$\frac{i_s}{\theta} = R \left(\frac{dI_o}{d\theta}\right)_{\theta=o}$$

For the incoherent case, this is

$$\frac{1}{\theta} i_s = R I_1 \frac{(1-K)^4 (1+K^4)}{(1-K^4)^2} (1-e_a^2) \sin 2\theta_o \qquad \text{(F-11)}$$

For the coherent case:

$$\frac{1}{\theta} i_s = R I_1 \frac{(1-K)^4 (1+K^2)}{(1-K^2)^3} (1-e_a^2) \sin 2\theta_o \qquad \text{(F-12)}$$

The detector current signal to noise ratio per unit of θ is, for an incoherent source and considering shot noise only,

$$\frac{1}{\theta}\,\frac{i_s}{i_n} = \left(\frac{RI_1}{e\Delta f}\right)^{1/2} \frac{(1-K)^{1/2}(1+K^4)}{(1+K^2)^{3/2}(1+K)^{3/2}}\,(1-e_a^{\,2})\,\frac{\sin 2\theta_o}{[1+e_a^{\,2}-(1-e_a^{\,2})\cos 2\theta_o]^{1/2}} \qquad \text{(F-13)}$$

By trigonometric identities this expression can be rewritten as

$$\frac{1}{\theta}\left(\frac{i_s}{i_n}\right) = \left(\frac{1}{2}\right)\frac{(1-K)^{\frac{1}{2}}(1+K^4)}{(1+K^2)^{3/2}(1+K)^{3/2}}\,(1-e_a^{\,2})\left(\frac{2RI_1}{e\Delta f}\right)^{\frac{1}{2}}\frac{\sin 2\theta_o}{[\sin^2\theta_o+e_a^{\,2}\cos^2\theta_o]^{1/2}} \qquad \text{(F-14)}$$

A similar calculation for the simple polarizer - analyzer system without mirrors gives a signal to noise ratio per unit θ of

$$\frac{1}{\theta}\left(\frac{i_s}{i_n}\right) = \frac{1}{2}\,(1-e_a^{\,2})\left(\frac{2RI_1}{e\Delta f}\right)^{\frac{1}{2}}\frac{\sin 2\theta_o}{[\sin^2\theta_o+e_a^{\,2}\cos^2\theta_o]^{1/2}} \qquad \text{(F-15)}$$

When this expression is compared with Eq. F-14, it is seen that the two are identical except for a factor in K appearing in Eq. F-14. This factor in K represents the effect of using mirrors. This factor is less than one for any value of reflectivity $0 < K \leq 1$, and is equal to unity only at K=0. This indicates that the sensitivity is better without mirrors for the incoherent case. Physically this means that the effect of the mirrors in attenuating the light as it is transmitted through them more than compensates for the increased effective length of the transmission path due to the reflections.

For a coherent light source of the proper frequency, the signal to noise ratio per unit θ is found from Eqs. F-10 and F-12 as

$$\frac{1}{\theta}\left(\frac{i_s}{i_n}\right) = \frac{1}{2}\left(\frac{2RI_1}{e\Delta f}\right)^{1/2}\frac{(1+K^2)}{(1+K)^2}\,(1-e_a^{\,2})\,\frac{\sin 2\theta_o}{(\sin^2\theta_o+e_a^{\,2}\cos^2\theta_o)^{1/2}} \qquad \text{(F-16)}$$

The factor in Eq. F-15 involving the reflectivity is again less than unity for all values of K greater than zero, so that the use of mirrors decreases the sensitivity.

Equations F-14 and F-16, when compared with F-15, shows that for a source of moderate power level (e. g., 100 watts plus losses) no improvement is obtained from the use of mirrors at the ends of the transmission path, if it is necessary that the light beam be transmitted through the reflecting surfaces of both mirrors.

Another reflecting configuration that might be used involves transmitting the light beam into the crystal through a small non-reflecting opening in the mirror surface, and aiming the beam so that it is reflected obliquely from a mirror at the output end and returns to strike the input mirror close to the non-reflecting aperture. The beam would then rebound back and forth through the crystal several times, finally reaching a small non-reflecting aperture in the output mirror and passing on to the detector. Since it would not be necessary to transmit the beam through reflecting portions of the mirrors, the input light intensity necessary to saturate the detector is practically the same as for the arrangement without mirrors. The increase in input power required to allow for reflection losses at the mirrors and increased absorption and side-scattering within the crystal is probably quite small with respect to the initial 100 watts required by the nearly-crossed polarizers, so it will be assumed that the light source could still be adjusted so as to saturate the detector. The net effect of the mirrors, then, is to increase the effective length of the crystal. This results in an angular rate theshold decreased by a factor equal to the number of trips the light beam makes between input and output mirrors. This number of "bounces" is limited by the beam width and angle of the source, the effect of the crystal in spreading the beam, and the width of a crystal face. Assuming that a beam of the necessary power level could be obtained with a width of one millimeter, and ignoring the beam spreading effects, a crystal width of two centimeters would allow about 35 trips between the mirrors. This would decrease the minimum detectable magnetic field of Chapter II to about 2×10^{-10} oersted, and the minimum detectable angular rate to about 1.5×10^{-3} radian per second, or about 20 earth rates.

This estimate of minimum detectable magnetic field strength, 10^{-10} oersted, is considerably better than the sensitivity that can be obtained from currently available magnetometers. This results from consistently making optimistic estimates of the parameters involved, and from completely

neglecting some factors, such as noise introduced from mechanical vibration of the polarizer and analyzer and noise generated in the associated electronics, which were not regarded as truly fundamental limitations but which would affect the performance of a practical instrument.

APPENDIX G

USE OF LASER AS LIGHT SOURCE

A laser has three characteristics that would make it particularly suitable for use as a light source in the optical systems described in Chapter II and IV and in Appendices E and F:

1. The output is linearly polarized and well collimated.
2. The output is coherent and monochromatic.
3. The peak power output of a pulsed unit can be very high.

The linear polarization of a laser output would allow the elimination of the polarizer. Similarly, the collimating lenses necessary for an ordinary source could be eliminated if a laser were used, so that a laser source would considerably simplify the optical system.

A coherent, monochromatic source would be essential for the use of interferometric techniques, and in fact a source with the general characteristics of a laser was tacitly assumed in Appendix F, in the discussion of the coherent case.

In Appendix F, the detector current signal to (shot) noise ratio per unit θ for a coherent source was calculated as

$$\frac{1}{2}\left(\frac{i_s}{i_n}\right) = \frac{1}{2}\left(\frac{2RI_1}{e\Delta f}\right)^{1/2} \frac{(1+K^2)}{(1+K)^2} \quad (1-e_a^{\,2}) \quad \frac{\sin 2\theta_o}{(\sin^2\theta_o + e_a^{\,2}\cos^2\theta_o)^{1/2}} \qquad \text{(F-15)}$$

For a source which provides W joules per pulse at a pulse width of Δt seconds, the average light intensity during a pulse, I_1, is $\frac{W}{\Delta t}$ watts. The bandwidth Δt that provides best signal to noise ratio is then around $\frac{W}{\Delta t}$ cps.[29] A bandwidth of at least ten cps was assumed to be required by the other equipment connected to the instrument, during the calculations for a continuous source; therefore, if the laser pulse width is one tenth of a second or more the appropriate value for Δt in Eq. F-15 is ten cps, and the sensitivity is improved by the square root of the ratio of laser peak power to the

power obtainable from a conventional source, neglecting the factor in K. If a laser with a pulse length as long as one tenth of a second could be built, its peak power would probably not greatly exceed the continuous power output of a conventional (noncoherent) source. Compared with Eq. E-13 for the conventional source without mirrors, the use of a pulsed laser source of pulse width of one tenth of a second or more would not improve the sensitivity by more than a factor of about two or three either with or without mirrors.

For shorter output pulses, it is possible to obtain increased intensity. The size and complexity of a laser and its associated equipment is roughly determined by its output energy per pulse, W. Since for high intensity pulses of less than one tenth of a second duration the bandwidth of the associated signal processing equipment beyond the detector should be about $\frac{1}{\Delta t}$ cps, the signal to noise ratio is

$$\frac{1}{\theta}\ \frac{i_s}{i_n} = \frac{1}{2}\left(\frac{2RW}{e}\right)^{1/2} \frac{(1+K^2)}{(1+K)^2}\ (1-e_a^{\,2})\ \frac{\sin 2\theta_o}{(\sin^2\theta_o + e_a^{\,2}\cos^2\theta_o)^{1/2}} \qquad \text{(G-1)}$$

Comparing this expression with Eq. E-13 for a continuous, incoherent, randomly polarized source without mirrors, it appears that the use of a pulsed laser with mirrors would improve the sensitivity by a factor of $(\frac{2W\Delta f}{I_1})^{1/2}$ $\frac{(1+K^2)}{(1+K)^2}$. It was assumed previously that $\frac{I_1}{\Delta f}$ would have a maximum practical value of about 10 joules per cycle. Assuming a laser with an output of 50 joules per pulse might be used, and neglecting the factor in K, an improvement of about a factor of three would be obtained in the signal to noise ratio. It is assumed in these calculations that the reflectivity of the mirrors is adjusted as a function of the laser peak power so that the detector remains just under saturation during a pulse. The necessary relation is given in Eq. F-8, with $I_b \leq I_{sat}$.

The improvement in sensitivity that could be derived from the use of a laser either with or without mirrors in the "interferometer" arrangement where the light beam must pass through reflecting surfaces of both mirrors, is probably limited to a factor of two or three.

In the second arrangement considered in Appdenix F, where the beam passes in and out of the crystal through non-reflecting apertures in the mirrors, a laser source does not provide any additional advantages not already assumed in Appendix F. However, a laser might well be necessary in order to provide a one millimeter beam of sufficient power, and with a very small beam angle.

BIBLIOGRAPHY

1. Ingersoll and Liebenberg, "Faraday Effect in Gases and Vapors," in three parts, Journal of the Optical Society of America, Vol. 44, page 566; Vol. 46, page 538; Vol. 48, page 339.

2. International Critical Tables, Vol. VI, page 425, (1929).

3. Chemical Rubber Co., Handbook of Chemistry and Physics, (35th edition).

4. Becquerel, DeHaas and Van DenHandel, Leiden Communications, Nr. 244, (1936-1938).

5. Becquerel and De Haas, Leiden Communications, Supplement 74a, (1932).

6. Becquerel and DeHaas, Leiden Communications, Nr. 199, (1929).

7. Alers, "Faraday Effect in Cerium Phosphate Glasses at Low Temperatures," Physical Review, Vol. 116, p. 1483, (1959).

8. Walton and Moss, "Free Carrier Faraday Effect in n-type Germanium," Journal of Applied Physics, Vol. 30, p. 951, (1959).

9. Spitzen and Fan, "Determination of Optical Constants and Carrier Effective Mass of Semiconductors," Physical Review, Vol. 106, p. 882, (1957).

10. Dillon, J. F., "Optical Properties of Several Ferrimagnetic Garnets," Journal of Applied Physics, Vol. 29, p. 539, (1958).

11. Sherwood, Remeika, and Williams, "Domain Behavior in Some Transparent Magnetic Oxides," Journal of Applied Physics, Vol. 30, p. 217, (1958).

12. Fowler and Fryer, "Magnetic Domains in Thin Films by the Faraday Effect," Physical Review, Vol. 104, p. 552, (1956).

13. Williams, Sherwood, Foster and Kelley, "Magnetic Writing on Thin Films of Mn Bi," Journal of Applied Physics, Vol. 28, p. 1181, (1957).

14. Barnett, S. J., "Magnetization by Rotation," Physical Review, Vol. 6, p. 239 (1915).

BIBLIOGRAPHY (continued)

15. Barnett, S. J. and Barnett, L. J. H., "New Researches on the Magnetization of Ferromagnetic Substances by Rotation and the Nature of the Elementary Magnet," Proceedings of the AAAS, Vol. 60, p. 27 (1925).

16. Barnett, S. J., "Gyromagnetic and Electron-inertia Effects," Reviews of Modern Physics, Vol. 7, p. 129 (1935).

17. Hogan, C. L., "The Ferromagnetic Faraday Effect at Microwave Frequencies and its Applications," Bell System Technical Journal, Vol. 31, p. 1 (1952).

18. Allen, P. J., "A Microwave Magnetometer," Proceedings of the IRE, Vol. 41, p. 100 (1953).

19. Faraday, M., "On the Magnetization of Light and the Illumination of Magnetic Lines of Force," Philosophical Transactions, 1846, p. 1

20. Houstoun, R. A., A Treatise on Light, Longmans, Green and Co. (1930).

21. Schuster and Nicholson, Theory of Optics, Edward Arnold and Co. (1928).

22. Becquerel and DeHaas, Leiden Communications, Supplement 81a (1936).

23. Rowen, J. H., "Ferrites in Microwave Applications," Bell System Technical Journal, Vol. 32, p. 1333 (1953).

24. Went and Gorter, "The Magnetic and Electrical Properties of Ferroxcube Materials," Philips Technical Review, Vol. 13, p. 181 (1952).

25. Palache, Berman, and Frondel, Dana's System of Mineralogy, Wiley, (1944).

26. DuMont Laboratories, Inc., DuMont Multiplier Phototubes (Technical Bulletin).

27. Reich, Ordung, Krauss and Skalnik, Microwave Theory and Techniques, Van Nostrand, p. 221 (1953).

28. Moss, Smith and Taylor, "The Infrared Faraday Effect due to Free Carriers in Indium Antimonide," Physics and Chemistry of Solids, Vol. 8, p. 323 (1959).

29. M.I.T. Radiation Laboratory Series, Vol. 23, Microwave Receivers.

Aeronautical Systems Division, Dir/Avionics, Navigation and Guidance Lab, Wright-Patterson AFB, Ohio. Rpt No. ASD-TDR-62-492, Vol I. THEORETICAL INVESTIGATION OF A MAGNETO-OPTICAL GYROSCOPE: Faraday and Transit-time Effects. Final report, Feb 63, 65p. incl illus., tables, 29 refs.

Unclassified Report

This report presents a study of magneto-optical and other closely related phenomena. The object of this study is to determine the sensitivity of these phenomena to angular motion in order to ascertain the feasibility of a "magneto-optical gyroscope."

The three phenomena studied are: (1) the optical Faraday effect, (2) the microwave Faraday effect, and (3) transit-time effects. Angular motion sensing instruments would utilize either of the first two effects in combination with the third. Throughout

(over)

these studies it is assumed that the output signal is generated in response to the rotation of the plane of polarization of the detected radiation relative to that of the incident radiation.

It is found that the transit-time effects produce little rotation of the plane polarization, for a given angular rate, compared with that produced by the Faraday effect. Estimates for angular motion sensors that employ the optical and microwave Faraday effects show that the resolutions that could be expected, after considerable development, would be of the order of 0.1 radian per second. To get this resolution magnetic fields must be shielded from the device so that field fluctuations are kept down to the order of 10^{-9} gauss. In view of this low resolution and high sensitivity to stray magnetic fields, "magneto-optical gyroscopes" based on the Faraday effect do not seem to be a fruitful area for further research.

1. Inertial guidance
2. Gyroscopes
I. AFSC Project 4431, Task 443124
II. Contract AF33(616)-7668
III. Electronic Systems Lab, Department of Electrical Engineering, Massachusetts Institute of Technology, Cambridge 39, Mass.
IV. Richard B. Rothrock
V. ESL-R-125(I)
VI. Aval fr OTS
VII. In ASTIA collection

Aeronautical Systems Division, Dir/Avionics, Navigation and Guidance Lab, Wright-Patterson AFB, Ohio. Rpt No. ASD-TDR-62-492, Vol I. THEORETICAL INVESTIGATION OF A MAGNETO-OPTICAL GYROSCOPE: Faraday and Transit-time Effects. Final report, Feb 63, 65p. incl illus., tables, 29 refs.

Unclassified Report

This report presents a study of magneto-optical and other closely related phenomena. The object of this study is to determine the sensitivity of these phenomena to angular motion in order to ascertain the feasibility of a "magneto-optical gyroscope."

The three phenomena studied are: (1) the optical Faraday effect, (2) the microwave Faraday effect, and (3) transit-time effects. Angular motion sensing instruments would utilize either of the first two effects in combination with the third. Throughout

(over)

these studies it is assumed that the output signal is generated in response to the rotation of the plane of polarization of the detected radiation relative to that of the incident radiation.

It is found that the transit-time effects produce little rotation of the plane polarization, for a given angular rate, compared with that produced by the Faraday effect. Estimates for angular motion sensors that employ the optical and microwave Faraday effects show that the resolutions that could be expected, after considerable development, would be of the order of 0.1 radian per second. To get this resolution magnetic fields must be shielded from the device so that field fluctuations are kept down to the order of 10^{-9} gauss. In view of this low resolution and high sensitivity to stray magnetic fields, "magneto-optical gyroscopes" based on the Faraday effect do not seem to be a fruitful area for further research.

1. Inertial guidance
2. Gyroscopes
I. AFSC Project 4431, Task 443124
II. Contract AF33(616)-7668
III. Electronic Systems Lab, Department of Electrical Engineering, Massachusetts Institute of Technology, Cambridge 39, Mass.
IV. Richard B. Rothrock
V. ESL-R-125(I)
VI. Aval fr OTS
VII. In ASTIA collection